Learning and Nonlinear Models (L&NLM) - Journal of the Brazilian Society on Neural Networks, Vol. 8, Iss. 2, pp. 71-92, 2010

MIMO VOLTERRA MODELING FOR NONLINEAR COMMUNICATION CHANNELS

Carlos Alexandre Rolim Fernandes
Federal University of Ceará, Computer Engineering
rua Anahid Andrade 472, 62011-000, Sobral, Brazil
carlosalexandre@deti.ufc.br

João Cesar Moura Mota
Federal University of Ceará, Dept. of Teleinformatics Engineering
Campus do Pici, 60.755-640, 6007 Fortaleza, Brazil
mota@gtel.ufc.br

Gérad Favier
I3S Laboratory, University of Nice-Sophia Antipolis, CNRS
2000 route des Lucioles, BP 121, 06903, Sophia Antipolis Cedex, France
favier@i3s.unice.fr

Abstract – Multiple-input multiple-output (MIMO) Volterra models have applications in different areas, including telecommunications. An overview of the modeling of nonlinear communication channels using MIMO Volterra models is presented in this paper. First, the development of an equivalent baseband discrete-time representation of a single-input single-output (SISO) Volterra system is carried out. This development constitutes the basis for several versions of discrete-time equivalent baseband MIMO Volterra systems presented in the sequel. The spectral broadening provided by a Volterra system on the equivalent baseband received signals is shown by calculating the frequency domain representation of the Volterra channel output. Some important block structured nonlinear MIMO models are also described, with their link to MIMO Volterra models. Finally, some applications of such models for communication systems are briefly discussed.

Keywords – MIMO systems, communication systems, nonlinear modeling, Volterra models, Wiener models, Hammerstein models.

Resumo – Os sistemas MIMO Volterra são poderosas ferramentas utilizadas na modelagem de sistemas não-lineares, possuindo aplicações em diferentes domínios, incluindo as telecomunicações. Este artigo apresenta uma visão geral sobre a modelagem de canais de comunicação não-lineares utilizando-se modelos MIMO Volterra. Inicialmente, uma representação em banda-base equivalente e tempo discreto é desenvolvida para um sistema SISO Volterra. Este desenvolvimento constitui a base para as versões de sistemas MIMO Volterra em banda-base equivalente e tempo discreto apresentadas na seqüência. O espalhamento espectral gerado por um sistema de Volterra nos sinais recebidos em banda de base é mostrado através do desenvolvimento da uma expressão para estes sinais no domínio da freqüência. Alguns modelos de sistemas MIMO não-lineares constituídos de cascatas em série de blocos lineares e não-lineares também são descritos, assim como suas relações com os sistemas MIMO Volterra. Ademais, algumas aplicações de modelos MIMO Volterra em sistemas de comunicações são discutidas no final do artigo.

Palavras-chave – Sistemas MIMO, sistemas de comunicação, modelos não-lineares, modelo de Volterra, modelo de Wiener, modelo de Hammerstein.

1. INTRODUCTION

An overview of the modeling of nonlinear communication channels using multiple-input multiple-output (MIMO) Volterra models is presented in this paper. The Volterra series [1], developed by the italian mathematician Vito Volterra in 1887, is one of the most common representations of nonlinear systems [2]. It constitutes a class of polynomial models that can be viewed as an extension of the linear convolution. The Volterra series have received a considerable attention from researchers of different areas. Among them, it should be highlighted the work of N. Wiener, on the modeling of nonlinear systems using Volterra series [3]. A main property of this kind of model is that it is linear with respect to its parameters. Another great advantage is its ability of modeling the behavior of nonlinear real-life phenomena, specially its ability to capture "memory" effects. Due to this characteristic, applications of Volterra models can be encountered in many areas as, for instance, in biological and physiological systems [4–6], magnetic recording channels [7] and engine transmission modeling [8].

Volterra models also have many applications in the field of telecommunication. Indeed, due to the presence of nonlinear devices such as power amplifiers (PA) and optical instruments, communication channels are sometimes corrupted by nonlinear

distortions such as nonlinear intersymbol interference (ISI), multiple access interference (MAI) and inter-carrier interference (ICI). These nonlinear distortions can significantly deteriorate the signal reception, leading to poor system performance. In such cases, linear models fail to characterize the communication channel, providing inexact channel description. Volterra models can then be used to provide an accurate channel representation, allowing the development of efficient signal processing techniques capable of eliminating or reducing these nonlinear distortions.

The Volterra model has since longtime being used to represent communication channels in presence of nonlinear distortions. One of the most important works in this subject is due to Benedetto *et al* [9], about the modeling and performance evaluation of satellite communication links with nonlinear PAs using Volterra series. Posterior works of S. Benedetto and E. Biglieri have significantly contributed to the modeling, estimation and equalization of nonlinear channels using Volterra models, mainly in the case of satellite communication channels [10–12]. Other important works about nonlinear satellite communication channels can be found in [13–17]. In fact, all the systems employing PAs are subject to nonlinear distortions that can be modeled as Volterra models. Orthogonal frequency division multiplexing (OFDM) signals are especially vulnerable to PA nonlinear distortions [18–24], as well as radio-over-fiber (ROF) communication systems [25–28]. Volterra models are also used for modelling ultra-wideband (UWB) systems [29, 30], nonlinear acoustic echo paths [31–33], software-defined radio systems [34], code division multiple access (CDMA) systems [35–37], etc. See [6] for more bibliography about applications of nonlinear models in communication systems.

Nevertheless, most of the works that use Volterra models for communication channels consider the case of single-input single-output (SISO) systems, and only a few works deal with nonlinear MIMO communication channels. In this paper, we consider that the multiple-inputs of a MIMO system represent various sources transmitting at the same time and frequency band, which may correspond to multiple users or a single user with multiple transmit antennas. On the other hand, the multiple-outputs represent the observations at the receiver obtained through an antenna array. In fact, the multiple observations at the receiver can also be obtained by oversampling the received signals, however, this approach is not considered in this paper. As well as in SISO communication channels, MIMO channels are subject to nonlinear distortions due to the presence of nonlinear blocks such as radio frequency PA and optical devices. Nonlinear MIMO communication channels can be found in OFDM systems [38, 39], multiuser ROF systems [27, 28, 40], satellite systems [28], CDMA systems [36], wireless communication links [20] and in ultra-wide-band systems [30].

When the received signals are nonlinear mixtures of transmitted signals, possibly including their delayed versions, MIMO Volterra models are interesting tools to model the communication channel. Different versions of MIMO Volterra models can be defined, depending on the generality of the model. Some versions of MIMO Volterra models have been used by a number of authors in different areas [8, 41–43]. However, to the best of our knowledge, few authors have used MIMO Volterra models in the context of communications systems [30, 36, 38, 39]. Moreover, the systems considered in these works do not correspond to the most general form of the MIMO Volterra model presented in this paper. Besides, multiple-input-single-output (MISO) Volterra models were used in [27, 28, 40], while single-input-multiple-output (SIMO) Volterra models were used in [44–46].

For simplifying this overview of nonlinear communication channels using Volterra models, we first consider the SISO case. Starting from the continuous-time passband received signal, we derive the expression of the continuous-time equivalent baseband received signal. In order to show the broadening of the spectral support provided by the Volterra system on the equivalent baseband received signal, the frequency domain representation of the Volterra channel is developed. The expression for the discrete-time equivalent baseband received signal is also introduced, constituting the basis for the development of MIMO Volterra models. An important property of these models is that their output is linear with respect to the system parameters, which allows to write the input-output relationship in a vector form.

At the end of the paper, we briefly present three applications of MIMO Volterra models for communication channels: OFDM, satellite and ROF systems. An interesting issue about these systems is that they can be modeled as block-structured nonlinear systems, i.e. series-cascades of nonlinear and linear blocks, such as MIMO Wiener, Hammerstein and Wiener-Hammerstein models. As it will be shown later, this kind of systems can be viewed as special cases of MIMO Volterra systems.

The rest of the paper is organized as follows. Section 2 presents the modeling of communication channels using SISO Volterra models. In Section 3, the discrete-time equivalent baseband MIMO Volterra models are introduced. Section 4 describes some MIMO systems constituted of series-cascades of linear and nonlinear blocks. Section 5 describes some applications of MIMO Volterra models for communication systems and the conclusions are drawn in Section 6.

2. SISO Volterra communication channels

The main Volterra models for SISO communication channels are introduced in this section, as well as some of their properties. The output $\check{x}(\xi)$ of a real-valued continuous-time SISO Volterra system of finite order $\check{K}$ can be represented by the the following input-output relationship:

$$\check{x}(\xi) = \sum_{k=1}^{\check{K}} \int_{-\infty}^{\infty} \cdots \int_{-\infty}^{\infty} \check{h}_k(\tau_1, \ldots, \tau_k) \prod_{i=1}^{k} \check{s}(\xi - \tau_i) d\tau_i \ , \tag{1}$$

where ξ is the continuous-time variable, $\check{h}_k(\tau_1, \ldots, \tau_k)$ is the real-valued continuous-time Volterra kernel of order k and $\check{s}(\xi)$ is the real-valued continuous-time input signal. One of the main advantages of the Volterra model is that it can be used for modeling a wide range of practical physical systems. Indeed, any finite memory causal and time-invariant nonlinear system can

be approximated by (1) [47]. It must be remarked that, when $\breve{K} = 1$, the Volterra model is equivalent to the convolution of the input signal with the linear kernel $\breve{h}_1(\tau_1)$.

A Volterra kernel $\breve{h}_k(\tau_1, \ldots, \tau_k)$ is said to be symmetric if it is invariant to any permutation of the indices $\tau_1, \ldots, \tau_k$. As a permutation of the indices $\tau_1, \ldots, \tau_k$ does not change the product $\prod_{i=1}^{k} \breve{s}(\xi - \tau_i)$, an asymmetric Volterra kernel can always be rewritten as a symmetric kernel [2]. For instance, let us consider a homogeneous Volterra system of order 2, i.e. a Volterra system containing only the quadratic real-valued kernel:

$$\breve{x}(\xi) = \int_{-\infty}^{\infty} \int_{-\infty}^{\infty} \bar{h}_2(\tau_1, \tau_2) \breve{s}(\xi - \tau_1) \breve{s}(\xi - \tau_2) d\tau_1 d\tau_2 \ , \tag{2}$$

where the kernel $\bar{h}_2(\tau_1, \tau_2)$ is non-symmetric, i.e. $\bar{h}_2(\tau_1, \tau_2) \neq \bar{h}_2(\tau_2, \tau_1)$. Equation (2) can be rewritten as

$$\breve{x}(\xi) = \int_{-\infty}^{\infty} \int_{-\infty}^{\infty} \breve{h}_2(\tau_1, \tau_2) \breve{s}(\xi - \tau_1) \breve{s}(\xi - \tau_2) d\tau_1 d\tau_2 \ , \tag{3}$$

with $\breve{h}_2(\tau_1, \tau_2) = (\bar{h}_2(\tau_1, \tau_2) + \bar{h}_2(\tau_2, \tau_1))/2$ being a symmetric kernel. In this paper, we assume that the Volterra kernels are symmetric with no loss of generality.

When (1) is used to model a communication channel, $\breve{x}(\xi)$ and $\breve{s}(\xi)$ can be viewed respectively as the bandpass received and transmitted signals. In the sequel, we derive the continuous- and discrete-time equivalent baseband representations of the Volterra system (1).

2.1 Equivalent baseband Volterra channel

The digital signal processing techniques for communications are generally based on discrete-time equivalent baseband representations of the received signals, which are obtained by sampling the continuous-time equivalent baseband received signals. The development of a continuous-time equivalent baseband Volterra system is then needed. A real-valued continuous-time bandpass signal $\breve{s}(\xi)$ and its continuous-time equivalent baseband version $s(\xi)$ are related by the following expression:

$$\begin{aligned} \breve{s}(\xi) &= \mathfrak{Re}\left\{ s(\xi) e^{\jmath\, 2\pi f_c \xi} \right\} \\ &= \frac{1}{2} \left[s(\xi) e^{\jmath\, 2\pi f_c \xi} + s^*(\xi) e^{-\jmath\, 2\pi f_c \xi} \right], \end{aligned} \tag{4}$$

where $\jmath = \sqrt{-1}$ is the imaginary unit, f_c the carrier frequency and $\mathfrak{Re}\{\cdot\}$ denotes the real part of the complex-valued argument. Let us assume that the baseband signal $s(\xi)$, also known as complex-envelope, is bandlimited, i.e. the Fourier transform and the power spectral density of $s(\xi)$ have finite support $I = [-B, B]$, B denoting the half of the signal bandwidth, assumed to be much smaller than f_c ($B \ll f_c$).

First, let us consider the case of a homogeneous Volterra system of order 2. Substituting (4) into (3), we get:

$$\begin{aligned} \breve{x}(\xi) = \frac{1}{4} \int_{-\infty}^{\infty} \int_{-\infty}^{\infty} \breve{h}_2(\tau_1, \tau_2) &\left[s(\xi - \tau_1) e^{\jmath\, 2\pi f_c (\xi - \tau_1)} + s^*(\xi - \tau_1) e^{-\jmath\, 2\pi f_c (\xi - \tau_1)} \right] \\ &\left[s(\xi - \tau_2) e^{\jmath\, 2\pi f_c (\xi - \tau_2)} + s^*(\xi - \tau_2) e^{-\jmath\, 2\pi f_c (\xi - \tau_2)} \right] d\tau_1 d\tau_2, \end{aligned} \tag{5}$$

which gives:

$$\begin{aligned} \breve{x}(\xi) &= \frac{1}{4} \int_{-\infty}^{\infty} \int_{-\infty}^{\infty} \breve{h}_2(\tau_1, \tau_2) \left[s(\xi - \tau_1) s(\xi - \tau_2) e^{\jmath\, 2\pi (2f_c) \xi} e^{\jmath\, 2\pi f_c (-\tau_1 - \tau_2)} \right. \\ &+ s(\xi - \tau_1) s^*(\xi - \tau_2) e^{\jmath\, 2\pi f_c (-\tau_1 + \tau_2)} + s^*(\xi - \tau_1) s(\xi - \tau_2) e^{\jmath\, 2\pi f_c (\tau_1 - \tau_2)} \\ &+ \left. s^*(\xi - \tau_1) s^*(\xi - \tau_2) e^{-\jmath\, 2\pi (2f_c) \xi} e^{\jmath\, 2\pi f_c (\tau_1 + \tau_2)} \right] d\tau_1 d\tau_2. \end{aligned} \tag{6}$$

At the receiver, the signal $\breve{x}(\xi)$ is filtered by a bandpass filter centered in f_c. Thus, if $B \ll f_c$, all the frequency components not centered at f_c are suppressed by the bandpass filter[1]. As we can see in (6), all the frequency components of $\breve{x}(\xi)$ are centered at the frequencies 0 and $2f_c$. This means that the received signal is equal to zero after the bandpass filter. In fact, it can be demonstrated that all the spectral components generated by even-order kernels are not centered at the carrier frequency f_c [48].

Similarly as (5), the output of a homogeneous Volterra system of order 3, i.e. a Volterra system containing only the cubic real-valued kernel, can be written as:

$$\begin{aligned} \breve{x}(\xi) = \frac{1}{8} \int_{-\infty}^{\infty} \int_{-\infty}^{\infty} \int_{-\infty}^{\infty} \breve{h}_3(\tau_1, \tau_2, \tau_3) &\left[s(\xi - \tau_1) e^{\jmath\, 2\pi f_c (\xi - \tau_1)} + s^*(\xi - \tau_1) e^{-\jmath\, 2\pi f_c (\xi - \tau_1)} \right] \\ &\left[s(\xi - \tau_2) e^{\jmath\, 2\pi f_c (\xi - \tau_2)} + s^*(\xi - \tau_2) e^{-\jmath\, 2\pi f_c (\xi - \tau_2)} \right] \\ &\left[s(\xi - \tau_3) e^{\jmath\, 2\pi f_c (\xi - \tau_3)} + s^*(\xi - \tau_3) e^{-\jmath\, 2\pi f_c (\xi - \tau_3)} \right] d\tau_1 d\tau_2 \tau_3, \end{aligned} \tag{7}$$

[1] In fact, bandpass filters can also be placed after nonlinear devices such as power amplifiers, in order to suppress all the frequency components lying outside the passband of the filter at this stage of the transmission.

or,equivalently,

$$\begin{aligned}\check{x}(\xi) &= \frac{1}{8}\int_{-\infty}^{\infty}\int_{-\infty}^{\infty}\int_{-\infty}^{\infty}\check{h}_3(\tau_1,\tau_2,\tau_3)\Big[s(\xi-\tau_1)s(\xi-\tau_2)s(\xi-\tau_3)e^{\jmath\,2\pi(3f_c)\xi}e^{\jmath\,2\pi f_c(-\tau_1-\tau_2-\tau_3)}\\ &+ s(\xi-\tau_1)s(\xi-\tau_2)s^*(\xi-\tau_3)e^{\jmath\,2\pi f_c\xi}e^{\jmath\,2\pi f_c(-\tau_1-\tau_2+\tau_3)} + s(\xi-\tau_1)s^*(\xi-\tau_2)s(\xi-\tau_3)e^{\jmath\,2\pi f_c\xi}e^{\jmath\,2\pi f_c(-\tau_1+\tau_2-\tau_3)}\\ &+ s(\xi-\tau_1)s^*(\xi-\tau_2)s^*(\xi-\tau_3)e^{-\jmath\,2\pi f_c\xi}e^{\jmath\,2\pi f_c(-\tau_1+\tau_2+\tau_3)} + s^*(\xi-\tau_1)s(\xi-\tau_2)s(\xi-\tau_3)e^{\jmath\,2\pi f_c\xi}e^{\jmath\,2\pi f_c(\tau_1-\tau_2-\tau_3)}\\ &+ s^*(\xi-\tau_1)s(\xi-\tau_2)s^*(\xi-\tau_3)e^{-\jmath\,2\pi f_c\xi}e^{\jmath\,2\pi f_c(\tau_1-\tau_2+\tau_3)} + s^*(\xi-\tau_1)s^*(\xi-\tau_2)s(\xi-\tau_3)e^{-\jmath\,2\pi f_c\xi}e^{\jmath\,2\pi f_c(\tau_1+\tau_2-\tau_3)}\\ &+ s^*(\xi-\tau_1)s^*(\xi-\tau_2)s^*(\xi-\tau_3)e^{-\jmath\,2\pi(3f_c)\xi}e^{\jmath\,2\pi f_c(\tau_1+\tau_2+\tau_3)}\Big]\,d\tau_1 d\tau_2\tau_3. \qquad (8)\end{aligned}$$

Note that the first and the last terms inside the brackets in (8) are centered at $3f_c$ and, consequently, they are suppressed by bandpass filtering. Thus, assuming that the kernel $\check{h}_3(\tau_1,\tau_2,\tau_3)$ is symmetric, we get the following expression for the bandpass received signal after the bandpass filter:

$$\begin{aligned}\bar{x}(\xi) = \frac{3}{8}\int_{-\infty}^{\infty}\int_{-\infty}^{\infty}\int_{-\infty}^{\infty}\check{h}_3(\tau_1,\tau_2,\tau_3)\Big[&s(\xi-\tau_1)s(\xi-\tau_2)s^*(\xi-\tau_3)e^{\jmath\,2\pi f_c(-\tau_1-\tau_2+\tau_3)}\\ &e^{\jmath\,2\pi f_c\xi} + s^*(\xi-\tau_1)s^*(\xi-\tau_2)s(\xi-\tau_3)e^{\jmath\,2\pi f_c(\tau_1+\tau_2-\tau_3)}e^{-\jmath\,2\pi f_c\xi}\Big]\,d\tau_1 d\tau_2\tau_3, \qquad (9)\end{aligned}$$

where we assumed that the bandpass filter is perfectly flat in the passband. Thus,

$$\bar{x}(\xi) = \mathfrak{Re}\left\{\left(\frac{3}{4}\int_{-\infty}^{\infty}\int_{-\infty}^{\infty}\int_{-\infty}^{\infty}\check{h}_3(\tau_1,\tau_2,\tau_3)s(\xi-\tau_1)s(\xi-\tau_2)s^*(\xi-\tau_3)e^{\jmath\,2\pi f_c(-\tau_1-\tau_2+\tau_3)}d\tau_1 d\tau_2\tau_3\right)e^{\jmath\,2\pi f_c\xi}\right\}. \qquad (10)$$

The equivalent baseband received signal is then given by:

$$x(\xi) = \int_{-\infty}^{\infty}\int_{-\infty}^{\infty}\int_{-\infty}^{\infty}h_3(\tau_1,\tau_2,\tau_3)s(\xi-\tau_1)s(\xi-\tau_2)s^*(\xi-\tau_3)d\tau_1 d\tau_3\tau_3, \qquad (11)$$

where

$$h_3(\tau_1,\tau_2,\tau_3) = \frac{3}{4}\check{h}_3(\tau_1,\tau_2,\tau_3)e^{\jmath\,2\pi f_c(-\tau_1-\tau_2+\tau_3)}. \qquad (12)$$

In a similar way, it can be shown that the equivalent baseband received signal for a Volterra system of order $2K+1$ can be written as [48]:

$$x(\xi) = \sum_{k=0}^{K}\int_{-\infty}^{\infty}\cdots\int_{-\infty}^{\infty}h_{2k+1}(\tau_1,\ldots,\tau_{2k+1})\prod_{i=1}^{k+1}s(\xi-\tau_i)\prod_{i=k+2}^{2k+1}s^*(\xi-\tau_i)d\tau_1 d\tau_2\ldots d\tau_{2k+1}, \qquad (13)$$

where the equivalent baseband kernel is given by:

$$h_{2k+1}(\tau_1,\ldots,\tau_{2k+1}) = \frac{C_{2k+1,k}}{2^{2k}}\;\check{h}_{2k+1}(\tau_1,\ldots,\tau_{2k+1})e^{\jmath 2\pi f_c(-\sum_{i=1}^{k+1}\tau_i+\sum_{i=k+2}^{2k+1}\tau_i)}. \qquad (14)$$

with $C_{i,p} = (i+p-1)!/(i-1)!p!$ denoting the number of combinations with repetition of p elements drawn from a set of i elements.

Three characteristics of the equivalent baseband Volterra system (13) should be highlighted. The first one is that it includes only the odd-order kernels with one more non-conjugated term than conjugated terms, the other terms being suppressed by the bandpass filter. The second one is that the Volterra coefficients (14) are complex-valued, while the bandpass Volterra coefficients in (1) are real-valued. The last one is that, due to the asymmetry of indices on the phase of the exponential term in (14): $\varphi(\tau_1,...,\tau_{2k+1}) = -\sum_{i=1}^{k+1}\tau_i + \sum_{i=k+2}^{2k+1}\tau_i$, the equivalent baseband Volterra kernels $h_{2k+1}(\tau_1,\ldots,\tau_{2k+1})$ are not symmetric.

2.2 Fourier transform of the Volterra channel output

The understanding of the behavior of a Volterra system can be improved in computing the spectrum of its output signal. In the sequel, the frequency domain representation of the equivalent baseband Volterra system (13) is developed. Using the inverse Fourier transform formula, we may rewrite (13) as:

$$\begin{aligned}x(\xi) = \sum_{k=0}^{K}\int_{-\infty}^{\infty}\cdots\int_{-\infty}^{\infty}h_{2k+1}(\tau_1,\ldots,\tau_{2k+1})\prod_{i=1}^{k+1}\left(\int_{-\infty}^{\infty}S(f_i)e^{\jmath\,2\pi f_i(\xi-\tau_i)}df_i\right)\\ \prod_{i=k+2}^{2k+1}\left(\int_{-\infty}^{\infty}S^*(-f_i)e^{\jmath\,2\pi f_i(\xi-\tau_i)}df_i\right)d\tau_1\ldots d\tau_{2k+1}, \qquad (15)\end{aligned}$$

where $S(f)$ denotes the Fourier transform of $s(\xi)$. Denoting by $H_{2k+1}(f_1,\ldots,f_{2k+1})$ the multidimensional Fourier transform of $h_{2k+1}(\tau_1,\ldots,\tau_{2k+1})$ given by:

$$H_{2k+1}(f_1,\ldots,f_{2k+1}) = \int_{-\infty}^{\infty}\cdots\int_{-\infty}^{\infty} h_{2k+1}(\tau_1,\ldots,\tau_{2k+1}) e^{-\jmath 2\pi\left(\sum_{i=1}^{2k+1} f_i\tau_i\right)} d\tau_1\ldots d\tau_{2k+1}, \tag{16}$$

equation (15) can be expressed as:

$$x(\xi) = \sum_{k=0}^{K}\int_{-\infty}^{\infty}\cdots\int_{-\infty}^{\infty} H_{2k+1}(f_1,\ldots,f_{2k+1}) \prod_{i=1}^{k+1} S(f_i) \prod_{i=k+2}^{2k+1} S^*(-f_i) e^{\jmath 2\pi\left(\sum_{i=1}^{2k+1} f_i\right)\xi} df_1\ldots df_{2k+1}. \tag{17}$$

Defining $\upsilon_i = \upsilon_{i-1} + f_i$, for $i = 1, 2, ..., 2k+1$, with $\upsilon_0 = 0$, (17) can be rewritten as:

$$x(\xi) = \int_{-\infty}^{\infty}\left(\sum_{k=0}^{K}\int_{-\infty}^{\infty}\cdots\int_{-\infty}^{\infty} H_{2k+1}(\upsilon_1, \upsilon_2-\upsilon_1,\ldots,\upsilon_{2k+1}-\upsilon_{2k}) \prod_{i=1}^{k+1} S(\upsilon_i-\upsilon_{i-1}) \prod_{i=k+2}^{2k+1} S^*(-(\upsilon_i-\upsilon_{i-1}))d\upsilon_1\ldots d\upsilon_{2k}\right) e^{\jmath 2\pi\upsilon_{2k+1}\xi} d\upsilon_{2k+1}. \tag{18}$$

Using

$$x(\xi) = \int_{-\infty}^{\infty} X(\upsilon_{2k+1}) e^{\jmath 2\pi\upsilon_{2k+1}\xi} d\upsilon_{2k+1}, \tag{19}$$

we get:

$$X(f) = \sum_{k=0}^{K}\int_{-\infty}^{\infty}\cdots\int_{-\infty}^{\infty} H_{2k+1}(\upsilon_1,\upsilon_2-\upsilon_1,\ldots,f-\upsilon_{2k}) \prod_{i=1}^{k+1} S(\upsilon_i-\upsilon_{i-1}) \prod_{i=k+2}^{2k} S^*(-(\upsilon_i-\upsilon_{i-1}))S^*(-(f-\upsilon_{2k})) d\upsilon_1\ldots d\upsilon_{2k}, \tag{20}$$

where $X(f)$ denotes the Fourier transform of $x(\xi)$ and υ_{2k+1} was replaced by f for the sake of simplifying the notation.

To get a better understanding of (20), let us consider a linear-cubic Volterra system ($K = 1$) and use the fact that $S(f)$ is zero outside $I = [-B, B]$:

$$X(f) = H_1(f)S(f) + \int_{-B}^{B}\int_{-2B}^{2B} H_3(\upsilon_1,\upsilon_2-\upsilon_1,f-\upsilon_2)S(\upsilon_1)S(\upsilon_2-\upsilon_1)S^*(-(f-\upsilon_2))d\upsilon_1 d\upsilon_2. \tag{21}$$

From (20), it can be concluded that the frequency support $X(f)$ is equal to $[-3B, 3B]$, which means that the output signal $x(\xi)$ may have spectral components outside the frequency support of the input signal $I = [-B, B]$.

It should be highlighted that a signal is never truly bandlimited in practice, as a bandlimited signal would require an infinite time support. Furthermore, due to causality, a system can not be truly bandlimited in practice neither. Thus, the bandwidth of a signal is usually considered as the range of frequencies where its Fourier transform has a power above a certain threshold. The signal bandwidth is then understood as the width of the frequency range where the main part of its power is located. Thus, when the envelope spectral broadening provided by the Volterra system is not important, the signal bandwidth may not change significantly.

Section 2.1 and present section show an important phenomenon caused by nonlinear channels called spectral broadening, which corresponds to spreading the spectrum of the transmitted signal. In fact, for a passband modulated signal, this phenomenon can be viewed as the sum of two different phenomena: the spectral broadening of the signal carrier and envelope. The broadening of the carrier implies that the received signal will have spectral components centered in frequencies different from the transmitted signal carrier. However, this phenomenon is canceled by using bandpass filters (zonal filters). On the other hand, the spectral broadening of signal envelope implies that the frequency support of the received signal envelope is higher than the frequency support of the transmitted signal envelope. This may lead to a significant increase of the signal bandwidth. The spectral broadening of the signal envelope can be partially canceled by a bandpass filter. However, sometimes it can be interesting to maintain all the spectral components of the signal envelope in order to exploit this information at the receiver.

Concerning the bandwidth of the bandpass filter considered in Section 2.1, two cases can be considered. The first one is when the bandpass filter bandwidth is wide enough to cover the spectral broadening provided by the Volterra system [13, 49]. In this case, it is generally assumed that the bandpass filter causes no significant signal distortion in the components centered at the frequency f_c, in such a way that this filter can be considered as transparent with respect to the equivalent baseband signal. The second case is when the bandpass filter bandwidth is not large enough to cover the spectral broadening, i.e. the bandpass filter partially rejects the nonlinear interference introduced by the Volterra filter at the frequency f_c [10, 50–52]. In this case, the bandpass filter can not be considered as transparent with respect to the equivalent baseband input signals.

2.3 Discrete-time equivalent baseband Volterra channel

A discrete-time representation of the equivalent baseband Volterra channel studied in Section 2.1 is developed in this section. Let us consider that the received signal (13) is sampled with a rate equal to W, assumed to be higher than or equal to the Nyquist rate $2B$ of the input signal. As pointed out earlier, a nonlinear system increases the signal bandwidth, which means that it is not possible to reconstruct the continuous-time channel output $x(\xi)$ from the discrete-time channel output $x(n)$ using a sampling rate of $W = 2B$. However, it was demonstrated that the Nyquist rate $2B$ of the input signal is sufficient to identify and compensate nonlinear systems [53, 54]. Indeed, the input signal sampled at the Nyquist rate $W = 2B$ leads to [55]:

$$S(f) = \sum_{n=-\infty}^{\infty} s(n) e^{-\jmath 2\pi n f/2B}. \tag{22}$$

In the sequel, the Volterra kernel $h_{2k+1}(\tau_1, \ldots, \tau_{2k+1})$ is assumed to be bandlimited, i.e. $H(f_1, ..., f_{2k+1}) = 0$ for $|f_i| > B$, $\forall i = 1, 2, ..., 2k+1$. In fact, from (20), it can be viewed that the form of $H(f_1, ..., f_{2k+1})$ outside the hypercube $I \times \cdots \times I$ ($I = [-B, B]$) is of no consequence since $S(f)$ vanishes outside I [54]. Thus, sampling the Volterra kernel $h_{\,2k+1}(\tau_1, \ldots, \tau_{2k+1})$ along the first dimension with the Nyquist rate of input signal as:

$$h_{2k+1}(n, \tau_2, \ldots, \tau_{2k+1}) = \frac{1}{2B}\, h_{2k+1}(\tau_1, \tau_2, \ldots, \tau_{2k+1})|_{\tau_1 = \frac{n}{2B}}\,, \tag{23}$$

leads to:

$$H_{2k+1}(f, \tau_2, \ldots, \tau_{2k+1}) = \frac{1}{2B} \sum_{n=-\infty}^{\infty} h_{2k+1}(n, \tau_2, \ldots, \tau_{2k+1}) e^{-\jmath 2\pi n f/2B}. \tag{24}$$

Thus, sampling the Volterra kernel as:

$$h_{2k+1}(n_1, \ldots, n_{2k+1}) = \frac{1}{(2B)^{2k+1}}\, h_{2k+1}(\tau_1, \ldots, \tau_{2k+1})|_{\tau_1 = \frac{n_1}{2B}, \cdots, \tau_{2k+1} = \frac{n_{2k+1}}{2B}}\,, \tag{25}$$

leads to:

$$H_{2k+1}(f_1, ..., f_{2k+1}) = \frac{1}{(2B)^{2k+1}} \sum_{n_1=-\infty}^{\infty} \cdots \sum_{n_2=-\infty}^{\infty} h_{2k+1}(n_1, \ldots, n_{2k+1}) e^{-\jmath 2\pi \left(\sum_{i=1}^{2k+1} n_i f_i\right)/2B}. \tag{26}$$

From (17), (22) and (26), the output signal sampled at the Nyquist rate of input signal can be written as:

$$x(n) = \frac{1}{(2B)^{2k+1}} \sum_{k=0}^{K} \int_{-B}^{B} \cdots \int_{-B}^{B} \sum_{n_1=-\infty}^{\infty} \cdots \sum_{n_{2k+1}=-\infty}^{\infty} h_{2k+1}(n_1, \ldots, n_{2k+1}) e^{-\jmath 2\pi \left(\sum_{i=1}^{2k+1} n_i f_i\right)/2B}$$
$$\prod_{i=1}^{k+1} \sum_{n_i^{'}=-\infty}^{\infty} s(n_i^{'}) e^{-\jmath 2\pi n_i^{'} f_i/2B} \prod_{i=k+2}^{2k+1} \sum_{n_i^{'}=-\infty}^{\infty} s^*(n_i^{'}) e^{\jmath 2\pi n_i^{'} f_i/2B} e^{\jmath 2\pi \left(\sum_{i=1}^{2k+1} f_i\right) n/2B} df_1 \ldots df_{2k+1}, \tag{27}$$

which leads to

$$x(n) = \frac{1}{(2B)^{2k+1}} \sum_{k=0}^{K} \sum_{n_1=-\infty}^{\infty} \cdots \sum_{n_{2k+1}=-\infty}^{\infty} h_{2k+1}(n_1, \ldots, n_{2k+1}) \int_{-B}^{B} \cdots \int_{-B}^{B} e^{-\jmath 2\pi \left(\sum_{i=1}^{2k+1} n_i f_i\right)/2B}$$
$$\sum_{n_1^{'}=-\infty}^{\infty} \cdots \sum_{n_{2k+1}^{'}=-\infty}^{\infty} \prod_{i=1}^{k+1} s(n_i^{'}) \prod_{i=k+2}^{2k+1} s^*(n_i^{'}) e^{-\jmath 2\pi \left(\sum_{i=1}^{2k+1} n_i^{'} f_i\right)/2B} e^{\jmath 2\pi \left(\sum_{i=1}^{2k+1} f_i\right) n/2B} df_1 \ldots df_{2k+1}, \tag{28}$$

or, yet,

$$x(n) = \frac{1}{(2B)^{2k+1}} \sum_{k=0}^{K} \sum_{n_1=-\infty}^{\infty} \cdots \sum_{n_{2k+1}=-\infty}^{\infty} \sum_{n_1^{'}=-\infty}^{\infty} \cdots \sum_{n_{2k+1}^{'}=-\infty}^{\infty} h_{2k+1}(n_1, \ldots, n_{2k+1}) \prod_{i=1}^{k+1} s(n_i^{'}) \prod_{i=k+2}^{2k+1} s^*(n_i^{'})$$
$$\prod_{i=1}^{2k+1} \int_{-B}^{B} e^{\jmath 2\pi \left(n - n_i - n_i^{'}\right) f_i/2B} df_i, \tag{29}$$

which implies:

$$x(n) = \sum_{k=0}^{K} \sum_{n_1=-\infty}^{\infty} \cdots \sum_{n_{2k+1}=-\infty}^{\infty} \sum_{n_1^{'}=-\infty}^{\infty} \cdots \sum_{n_{2k+1}^{'}=-\infty}^{\infty} h_{2k+1}(n_1, \ldots, n_{2k+1}) \prod_{i=1}^{k+1} s(n_i^{'}) \prod_{i=k+2}^{2k+1} s^*(n_i^{'})$$
$$\prod_{i=1}^{2k+1} \text{sinc}\left(\pi \left[n - n_i - n_i^{'}\right]\right), \tag{30}$$

where

$$\text{sinc}\,(\theta) = \begin{cases} 1, & \text{for} \quad \theta = 0 \\ \frac{\sin\theta}{\theta}, & \text{otherwise.} \end{cases} \tag{31}$$

Equation (30) can then be rewritten as:

$$x(n) = \sum_{k=0}^{K} \sum_{n_1=-\infty}^{\infty} \cdots \sum_{n_{2k+1}=-\infty}^{\infty} h_{2k+1}(n_1, \ldots, n_{2k+1}) \prod_{i=1}^{k+1} s(n-n_i) \prod_{i=k+2}^{2k+1} s^*(n-n_i). \tag{32}$$

The output $x(n)$ of a causal complex-valued discrete-time baseband equivalent Volterra system of finite memory M can then be represented by the following relationship:

$$x(n) = \sum_{k=0}^{K} \sum_{m_1=0}^{M} \cdots \sum_{m_{2k+1}=0}^{M} h_{2k+1}(m_1, \ldots, m_{2k+1}) \prod_{i=1}^{k+1} s(n-m_i) \prod_{i=k+2}^{2k+1} s^*(n-m_i). \tag{33}$$

Note that (33) corresponds to the output of a linear finite impulse response (FIR) filter of order $(M+1)$ when $K = 0$, the coefficients of which are given by the linear kernel $h_1(m_1)$, for $0 \leq m_1 \leq M$.

The discrete-time Volterra model (33) can be rewritten in a compact form as:

$$x(n) = \mathbf{h}^T \mathbf{w}(n), \tag{34}$$

where $\mathbf{w}(n) \in \mathbb{C}^{Q\times 1}$ is the nonlinear regression vector given by:

$$\mathbf{w}(n) = [\mathbf{s}^T(n) \;\; \otimes_*^3 \mathbf{s}^T(n) \;\; \cdots \;\; \otimes_*^{2K+1} \mathbf{s}^T(n)]^T, \tag{35}$$

with the operator $\otimes_*^{2k+1}$ defined as:

$$\otimes_*^{2k+1} \mathbf{s}(n) = \left[\otimes^{k+1} \mathbf{s}(n)\right] \otimes \left[\otimes^{k} \mathbf{s}^*(n)\right] \in \mathbb{C}^{(M+1)^{2k+1}\times 1}, \tag{36}$$

$\mathbf{s}(n) = [s(n) \; s(n-1) \; \ldots \; s(n-M)]^T \in \mathbb{C}^{(M+1)\times 1}$ being the linear regression vector, $\otimes^k \mathbf{s}(n)$ the power of order k of the Kronecker product of $\mathbf{s}(n)$ and Q the number of channel coefficients (nonlinear terms) of the Volterra filter, given by:

$$Q = \sum_{k=0}^{K} (M+1)^{2k+1}. \tag{37}$$

Note that $\mathbf{w}(n)$ contains all the products like $\prod_{i=1}^{k+1} s(n-m_i) \prod_{i=k+2}^{2k+1} s^*(n-m_i)$ of (33). Moreover, the vector $\mathbf{h} \in \mathbb{C}^{Q\times 1}$ containing the Volterra coefficients is given by:

$$\mathbf{h} = \left[\left(\mathbf{h}^{(1)}\right)^T \;\; \left(\mathbf{h}^{(3)}\right)^T \;\; \ldots \;\; \left(\mathbf{h}^{(2K+1)}\right)^T \right]^T, \tag{38}$$

with $\mathbf{h}^{(2k+1)} \in \mathbb{C}^{(M+1)^{2k+1}\times 1}$, for $0 \leq k \leq K$. Moreover, the q^{th} element of $\mathbf{h}^{(2k+1)}$ can be written as $h_q^{(2k+1)} = h_{2k+1}(m_1, \ldots, m_{2k+1})$, with

$$\begin{aligned} q &= m_{2k+1} + m_{2k}(M+1) + \cdots + m_2(M+1)^{2k-1} + m_1(M+1)^{2k} \\ &= \sum_{i=1}^{2k+1} m_i (M+1)^{2k+1-i}, \end{aligned} \tag{39}$$

for $0 \leq m_1, m_2, ..., m_{2k+1} \leq M+1$.

From (34), it can be viewed that the output $x(n)$ is linear with respect to the system parameters $h_{2k+1}(m_1, \ldots, m_k)$. This means that a Volterra filter can be viewed as a linear system where the output is a weighted sum of Q virtual-sources or quasi-sources, these sources being given by the nonlinear products $w_q(n)$ of the input, where $w_q(n)$ denotes the q^{th} element of the nonlinear regression vector $\mathbf{w}(n)$. In fact, this property corresponds to one of the main advantages of Volterra models, as it may simplify the estimation of the system coefficients and the recovery of the input signals.

2.4 Triangular form

Let us go back to the discrete-time baseband equivalent Volterra model (33). One of the main drawbacks of this model is its high number of coefficients. It can be viewed in (37) that the number of parameters Q grows exponentially with the nonlinearity

order $2K+1$. However, it can be noted that some terms of the nonlinear regression vector (35) are redundant. They can be eliminated by rewriting (33) as a triangular Volterra system:

$$x(n) = \sum_{k=0}^{K} \sum_{m_1=0}^{M} \sum_{m_2=m_1}^{M} \cdots \sum_{m_{k+1}=m_k}^{M} \sum_{m_{k+2}=0}^{M} \cdots \sum_{m_{2k+1}=m_{2k}}^{M} \tilde{h}_{2k+1}(m_1, m_2, \ldots, m_{2k+1}) \prod_{i=1}^{k+1} s(n-m_i) \prod_{i=k+2}^{2k+1} s^*(n-m_i). \quad (40)$$

with

$$\tilde{h}_{2k+1}(m_1, m_2, \ldots, m_{2k+1}) = \underbrace{\sum_{\tilde{m}_1=0}^{M} \cdots \sum_{\tilde{m}_{k+1}=0}^{M}}_{\substack{\{\tilde{m}_1,\ldots,\tilde{m}_{k+1}\}\in \\ \pi(m_1,\ldots,m_{k+1})}} \underbrace{\sum_{\tilde{m}_{k+2}=0}^{M} \cdots \sum_{\tilde{m}_{2k+1}=0}^{M}}_{\substack{\{\tilde{m}_{k+2},\ldots,\tilde{m}_{2k+1}\}\in \\ \pi(m_{k+2}\ldots,m_{2k+1})}} h_{2k+1}(\tilde{m}_1, \tilde{m}_2, \ldots, \tilde{m}_{2k+1}), \quad (41)$$

where $\pi(m_1, \ldots, m_{k+1})$ denotes the set of all the permutations of $\{m_1, \ldots, m_{k+1}\}$. Note that, in (40), we have $m_1 \leq \cdots \leq m_{k+1}$ and $m_{k+2} \leq \cdots \leq m_{2k+1}$.

The vector form of a triangular Volterra model is given by:

$$x(n) = \tilde{\mathbf{h}}^T \mathbf{w}(n), \quad (42)$$

where the nonlinear regression vector $\mathbf{w}(n) \in \mathbb{C}^{Q\times 1}$ is given by:

$$\mathbf{w}(n) = [\mathbf{s}^T(n) \;\; \oslash_*^3 \mathbf{s}^T(n) \;\cdots\; \oslash_*^{2K+1} \mathbf{s}^T(n)]^T \in \mathbb{C}^{Q\times 1}, \quad (43)$$

the operator $\oslash_*^{2k+1}$ being defined as:

$$\oslash_*^{2k+1} \mathbf{s}(n) = \left[\oslash^{k+1} \mathbf{s}(n)\right] \otimes \left[\oslash^{k} \mathbf{s}^*(n)\right] \quad (44)$$

and $\oslash^k \mathbf{s}(n)$ being the power of order k of the *truncated Kronecker product* of $\mathbf{s}(n)$ (see Appendix). The vector $\tilde{\mathbf{h}} \in \mathbb{C}^{Q\times 1}$ contains the parameters of the triangular Volterra model $\tilde{h}_{2k+1}(m_1, m_2, \ldots, m_{2k+1})$ and the number of parameters Q can be deduced from (85) in Appendix:

$$Q = \sum_{k=0}^{K} C_{M+1,k} C_{M+1,k+1}. \quad (45)$$

If the input signals have a constant modulus, as in Phase Shift Keying (PSK) modulations, the triangular Volterra model (40) can be rewritten with a smaller number of coefficients, as some power terms of $s(n)$ can be viewed as power terms of smaller order. Indeed, if $m_i = m_j$, for $i \in \{1, ..., k+1\}$ and $j \in \{k+2, ..., 2k+1\}$, the term $|s(n)|^2$ reduces to a multiplicative constant that can be absorbed by the associated channel coefficient. As a consequence, some nonlinear terms degenerate in terms of smaller order.

For instance, for constant modulus input signals with $|s(n)| = A$, the Volterra model (33) can be reexpressed as:

$$x(n) = \sum_{m_1=0}^{M} \underline{h}_1(m_1) s(n-m_1) + \sum_{m_1=0}^{M} \sum_{m_2=m_1}^{M} \sum_{\substack{m_3=0 \\ m_3\neq m_1, m_2}}^{M} \underline{h}_3(m_1, m_2, m_3) s(n-m_1) s(n-m_2) s^*(n-m_3), \quad (46)$$

where $\underline{h}_3(m_1, m_2, m_3) = \tilde{h}_3(m_1, m_2, m_3)$, for $0 \leq m_1 \leq m_2 \leq M$, $0 \leq m_3 \leq M$ and $m_3 \neq m_1, m_2$, and

$$\underline{h}_1(m_1) = \tilde{h}_1(m_1) + \sum_{\substack{\tilde{m}=0 \\ \tilde{m}\leq m_1}}^{M} \tilde{h}_3(\tilde{m}, m_1, \tilde{m}) A^2 + \sum_{\substack{\tilde{m}=0 \\ \tilde{m}> m_1}}^{M} \tilde{h}_3(m_1, \tilde{m}, \tilde{m}) A^2. \quad (47)$$

In this case, we have $Q = M + 1 + \frac{(M+1)^2 M}{2}$.

PSK signals provide then less nonlinear distortions than non-constant modulus signals, like quadrature amplitude modulation (QAM) signals, due to the fact that PSK symbols have less amplitude fluctuations than QAM symbols, which makes the use of PSK signals interesting for transmissions over nonlinear channels. The performance of PSK signals over nonlinear satellite channels was investigated by several authors [10, 13] and some properties of nonlinearly distorted PSK signals were established in [56].

3. MIMO Volterra channels

As well as SISO communication channels, MIMO channels are also subject to nonlinear distortions. In these cases, MIMO Volterra models can be used for providing an accurate description of the channel. Some applications of MIMO Volterra models for modeling communication systems are discussed in Section 5. The models described in the sequel correspond to the most general forms of MIMO Volterra systems, considering discrete-time equivalent baseband representations.

For developing the input-output relationship of a discrete-time equivalent baseband MIMO Volterra model, let us first consider a nonlinear single-input-multiple-output (SIMO) communication channel. That corresponds to the case where a single source transmits to an array of R receive antennas. The results presented in Section 2 for SISO Volterra models can be developed in a similar way for SIMO Volterra channels, the link between each antenna element and the source being modeled as the SISO discrete-time baseband equivalent Volterra system (33). Thus, the discrete-time signal received by the r^{th} antenna element can be expressed as:

$$x_r(n) = \sum_{k=0}^{K} \sum_{m_1=0}^{M} \cdots \sum_{m_{2k+1}=0}^{M} h_{2k+1}^{(r)}(m_1, \ldots, m_{2k+1}) \prod_{i=1}^{k+1} s(n-m_i) \prod_{i=k+2}^{2k+1} s^*(n-m_i). \tag{48}$$

where $h_{2k+1}^{(r)}(m_1, \ldots, m_{2k+1})$ are the Volterra kernels coefficients associated with the r^{th} output.

In the case of MIMO channel, if the link between each source (transmit antenna or user) and each receive antenna is modeled as a Volterra system, the r^{th} output signal is expressed by:

$$x_r(n) = \sum_{t=1}^{T} \sum_{k=0}^{K} \sum_{m_1=0}^{M} \cdots \sum_{m_{2k+1}=0}^{M} h_{2k+1}^{(r)}(t, m_1, \ldots, m_{2k+1}) \prod_{i=1}^{k+1} s_t(n-m_i) \prod_{i=k+2}^{2k+1} s_t^*(n-m_i). \tag{49}$$

where $s_t(n)$ is the t^{th} input signal ($1 \leq t \leq T$) and $h_k^{(r)}(t, m_1, \ldots, m_k)$ are the Volterra kernels coefficients associated with the r^{th} output and the t^{th} input signal.

Note that the discrete-time baseband equivalent MIMO Volterra system (49) have products of the input signals in the form $\prod_{i=1}^{k+1} s_t(n-m_i) \prod_{i=k+2}^{2k+1} s_t^*(n-m_i)$, which means that it does not contain products of different sources. This corresponds to the case where the signal of each source is corrupted by nonlinear ISI and, then, the signal of all the sources are linearly mixed, i.e. the nonlinearities are applied to the input signals individually, before mixing the sources. This kind of model can be viewed as a parallel-cascade of T SIMO Volterra systems. Thus, although (49) corresponds to a MIMO Volterra model, it does not represent the case where the sources are nonlinearly mixed. In order to develop a generical expression for a MIMO Volterra model taking this case into account, let us consider the SIMO Volterra system (48) with the input signal $s(n)$ being the mixture of T different sources:

$$s(n) = \sum_{t=1}^{T} a_t s_t(n), \tag{50}$$

leading to:

$$x_r(n) = \sum_{k=0}^{K} \sum_{m_1=0}^{M} \cdots \sum_{m_{2k+1}=0}^{M} h_{2k+1}^{(r)}(m_1, \ldots, m_{2k+1}) \prod_{i=1}^{k+1} \left(\sum_{t=1}^{T} a_t s_t(n-m_i) \right) \prod_{i=k+2}^{2k+1} \left(\sum_{t=1}^{T} a_t^* s_t^*(n-m_i) \right), \tag{51}$$

or, equivalently,

$$x_r(n) = \sum_{k=0}^{K} \sum_{t_1=1}^{T} \cdots \sum_{t_{2k+1}=1}^{T} \sum_{m_1=0}^{M} \cdots \sum_{m_{2k+1}=0}^{M} \left[h_{2k+1}^{(r)}(m_1, \ldots, m_{2k+1}) \prod_{i=1}^{k+1} a_{t_i} \prod_{i=k+2}^{2k+1} a_{t_i}^* \right] \prod_{i=1}^{k+1} s_{t_i}(n-m_i) \prod_{i=k+2}^{2k+1} s_{t_i}^*(n-m_i). \tag{52}$$

The MIMO Volterra model (52) contains products of different sources $\prod_{i=1}^{k+1} s_{t_i}(n-m_i) \prod_{i=k+2}^{2k+1} s_{t_i}^*(n-m_i)$, as it corresponds to the case where the nonlinearities are applied to the input signals after mixing the sources. Based on (52), the general discrete-time equivalent baseband MIMO Volterra model with T inputs and R outputs is defined as:

$$x_r(n) = \sum_{k=0}^{K} \sum_{t_1=1}^{T} \cdots \sum_{t_{2k+1}=1}^{T} \sum_{m_1=0}^{M} \cdots \sum_{m_{2k+1}=0}^{M} h_{2k+1}^{(r)}(t_1, \ldots, t_{2k+1}, m_1, \ldots, m_{2k+1}) \prod_{i=1}^{k+1} s_{t_i}(n-m_i) \prod_{i=k+2}^{2k+1} s_{t_i}^*(n-m_i). \tag{53}$$

where $h_{2k+1}^{(r)}(t_1, \ldots, t_{2k+1}, m_1, \ldots, m_k)$ are the Volterra kernels coefficients associated with the r^{th} output and the product $\prod_{i=1}^{k+1} s_{t_i}(n-m_i) \prod_{i=k+2}^{2k+1} s_{t_i}^*(n-m_i)$. When the diversity at the reception is provided by an antenna array, equation (53) can

be viewed as a "spatial-temporal Volterra" model in contrast with the "temporal Volterra" model (33). Indeed, in this case, the Volterra kernels have multiple time $(t_1, \ldots, t_k)$ and space $(m_1, \ldots, m_k)$ indices, instead of only time indices, as in the SISO Volterra system (33), or multiple time indices and only one space index, as in the MIMO Volterra model (49).

As well as for the SISO case, the discrete-time MIMO Volterra model (53) can be rewritten in a triangular form, in such a way that the redundant terms are eliminated:

$$x_r(n) = \sum_{k=0}^{K} \sum_{t_1=1}^{T} \cdots \sum_{t_{k+1}=t_k}^{T} \sum_{t_{k+2}=1}^{T} \cdots \sum_{t_{2k+1}=t_{2k}}^{T} \sum_{m_1=0}^{M} \cdots \sum_{m_{k+1}=m'_{k+1}}^{M} \sum_{m_{k+2}=0}^{M} \cdots \sum_{m_{2k+1}=m'_{2k+1}}^{M}$$
$$\tilde{h}^{(r)}_{2k+1}(t_1, \ldots, t_{2k+1}, m_1, \ldots, m_{2k+1}) \prod_{i=1}^{k+1} s_{t_i}(n - m_i) \prod_{i=k+2}^{2k+1} s^*_{t_i}(n - m_i). \tag{54}$$

with

$$m'_k = \begin{cases} m_{k-1} & \text{if} \quad t_k = t_{k-1}, \\ 0 & \text{if} \quad t_k \neq t_{k-1}, \end{cases} \tag{55}$$

It is also possible to define a MIMO Volterra model in order to take into account the fact that the system has different memories with respect to the inputs. Thus, a more general representation of discrete-time baseband equivalent MIMO Volterra systems can be written as:

$$x_r(n) = \sum_{k=0}^{K} \sum_{t_1=1}^{T} \cdots \sum_{t_{k+1}=t_k}^{T} \sum_{t_{k+2}=1}^{T} \cdots \sum_{t_{2k+1}=t_{2k}}^{T} \sum_{m_1=0}^{M_{t_1}} \cdots \sum_{m_{k+1}=m'_{k+1}}^{M_{t_{k+1}}} \sum_{m_{k+2}=0}^{M_{t_{k+2}}} \cdots \sum_{m_{2k+1}=m'_{2k+1}}^{M_{t_{2k+1}}}$$
$$\tilde{h}^{(r)}_{2k+1}(t_1, \ldots, t_{2k+1}, m_1, \ldots, m_{2k+1}) \prod_{i=1}^{k+1} s_{t_i}(n - m_i) \prod_{i=k+2}^{2k+1} s^*_{t_i}(n - m_i), \tag{56}$$

where M_{t_i} is the memory of the system with respect to the t_i^{th} input, for $1 \leq t_i \leq T$. The system model (56) can still be rewritten in a different way:

$$x_r(n) = \sum_{k=0}^{K} \sum_{\bar{m}_1=1}^{\bar{M}} \cdots \sum_{\bar{m}_{k+1}=\bar{m}_k}^{\bar{M}} \sum_{\bar{m}_{k+2}=1}^{\bar{M}} \cdots \sum_{\bar{m}_{2k+1}=\bar{m}_{2k}}^{\bar{M}} \tilde{h}^{(r)}_{2k+1}(\bar{m}_1, \ldots, \bar{m}_{2k+1}) \prod_{i=1}^{k+1} \bar{s}_{\bar{m}_i}(n) \prod_{i=k+2}^{2k+1} \bar{s}^*_{\bar{m}_i}(n), \tag{57}$$

where $\bar{M} = M_1 + \cdots + M_T + T$ and $\bar{s}_{\bar{m}_i}(n)$ corresponds to the $\bar{m}_i^{th}$ component of the linear input vector defined as:

$$\begin{aligned} \bar{\mathbf{s}}(n) &= [\bar{s}_1(n)\ \bar{s}_2(n)\ \ldots\ \bar{s}_{\bar{M}}(n)]^T \qquad \in \mathbb{C}^{\bar{M}\times 1} \\ &= [s_1(n) \ldots s_1(n - M_1) \cdots s_T(n) \ldots s_T(n - M_T)]^T . \end{aligned} \tag{58}$$

The Volterra models (56) and (57) are equivalent and can be represented in the following compact way:

$$\mathbf{x}(n) = \tilde{\mathbf{H}}\mathbf{w}(n), \tag{59}$$

where $\mathbf{x}(n) = [x_1(n)\ x_2(n) \ldots x_R(n)]^T \in \mathbb{C}^{R\times 1}$ and the nonlinear input vector $\mathbf{w}(n) \in \mathbb{C}^{Q\times 1}$ is given by:

$$\mathbf{w}(n) = [\bar{\mathbf{s}}^T(n) \ \oslash_*^3 \bar{\mathbf{s}}^T(n) \ \cdots \ \oslash_*^{2K+1} \bar{\mathbf{s}}^T(n)]^T \in \mathbb{C}^{Q\times 1}, \tag{60}$$

with $\bar{\mathbf{s}}(n)$ given by (58). Moreover, $\tilde{\mathbf{H}} = [\tilde{\mathbf{h}}_1\, \tilde{\mathbf{h}}_2 \ldots \tilde{\mathbf{h}}_R]^T \in \mathbb{C}^{R\times Q}$, with $\tilde{\mathbf{h}}_r \in \mathbb{C}^{Q\times 1}$ $(1 \leq r \leq R)$ containing the coefficients of the triangular Volterra system associated with r^{th} output. In this case, the length of the Volterra filter is given by:

$$Q = \sum_{k=0}^{K} C_{\bar{M},k} C_{\bar{M},k+1} \,. \tag{61}$$

Discrete-time MIMO Volterra models have being studied in a few works. However, some of these works deal with MIMO Volterra systems less generical than (53) [8, 30, 36, 38, 39, 41, 43], while some others deal with a real-valued version [42] or with a memoryless version of this model [57–62]. To the best of our knowledge, the techniques that we proposed in [63, 64] are only works that use the generical complex-valued equivalent baseband MIMO Volterra model (53). However, these works did not presented the above developments.

4. Block-structured nonlinear MIMO systems

Most nonlinear MIMO communication channels used in the literature are constituted of series-cascades of nonlinear and linear systems. In this section, three block-structured nonlinear systems are considered: the Wiener, Hammerstein and Wiener-Hammerstein systems. These block-structured nonlinear systems have important applications in many areas [65] and especially in telecommunication systems, as we will see in Section 5. The next developments concern discrete-time equivalent baseband MIMO models, the SISO case corresponding to $T = R = 1$.

It will be shown that these block-structured nonlinear systems can be viewed as particular cases of MIMO Volterra systems. One of the main advantages of these block-structured models is that they are characterized by less parameters than their associated Volterra representations. On the other hand, an important drawback of such kind of models is that they are not linear with respect to their parameters, contrarily to Volterra models.

4.1 The MIMO Wiener model

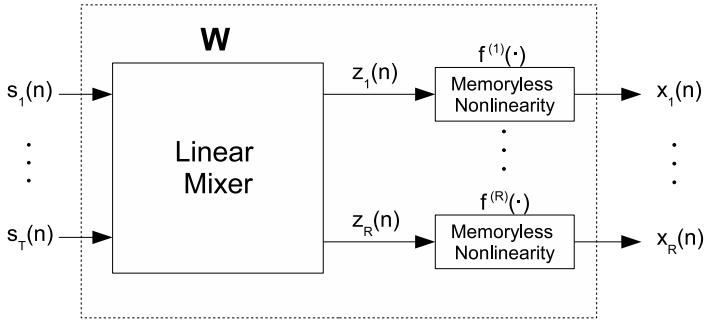

Figure 1: A MIMO Wiener system.

A SISO Wiener system is the cascade of a linear filter followed by a static nonlinearity. In its most general form, a MIMO Wiener system with T inputs and R outputs is composed of a linear convolutional mixer followed by memoryless nonlinearities, as shown in Fig. 1. Let us denote by $z_r(n)$ ($1 \leq r \leq R$) the outputs of the linear mixer and by $w_t^{(r)}(m)$ ($0 \leq m \leq M$) the $(m+1)^{th}$ element of the impulse response associated with the t^{th} input and the r^{th} output. It is considered that the system has the same memory M with respect to all inputs. Thus, we may write:

$$z_r(n) = \sum_{t=1}^{T} \sum_{m=0}^{M} w_t^{(r)}(m) s_t(n-m). \tag{62}$$

Denoting by $x_r(n)$ ($1 \leq r \leq R$) the outputs of the MIMO Wiener system, we have:

$$x_r(n) = f^{(r)}\left(z_r(n)\right), \tag{63}$$

where $f^{(r)}(\cdot)$ ($1 \leq r \leq R$) is a polynomial function. Considering an equivalent baseband representation, similarly as for the Volterra models (53)-(57), the functions $f^{(r)}(\cdot)$ can be represented by a polynomial of the form:

$$x_r(n) = \sum_{k=0}^{K} f_{2k+1}^{(r)} \left|z_r(n)\right|^{2k} z_r(n), \tag{64}$$

where $|\cdot|$ denotes the magnitude of a complex number and $\{f_1^{(r)}, f_3^{(r)}, \ldots, f_{2K+1}^{(r)}\}$ are the baseband equivalent coefficients of the polynomial function $f^{(r)}(\cdot)$. As in (53)-(57), the polynomial terms that do not have the form shown in (64) correspond to spectral components lying outside the system bandwidth.

Substituting (62) into (64), we get:

$$x_r(n) = \sum_{k=0}^{K} f_{2k+1}^{(r)} \left|\sum_{t=1}^{T} \sum_{m=0}^{M} w_t^{(r)}(m) s_t(n-m)\right|^{2k} \sum_{t=1}^{T} \sum_{m=0}^{M} w_t^{(r)}(m) s_t(n-m), \tag{65}$$

or, equivalently,

$$x_r(n) = \sum_{k=0}^{K} \sum_{t_1=1}^{T} \cdots \sum_{t_{2k+1}=1}^{T} \sum_{m_1=0}^{M} \cdots \sum_{m_{2k+1}=0}^{M} f_{2k+1}^{(r)} \prod_{i=1}^{k+1} w_{t_i}^{(r)}(m_i) s_{t_i}(n-m_i) \prod_{i=k+2}^{2k+1} \left[w_{t_i}^{(r)}(m_i) s_{t_i}(n-m_i)\right]^{*}. \tag{66}$$

Thus, by defining the following kernel:

$$h_{2k+1}^{(r)}(t_1,\ldots,t_{2k+1},m_1,\ldots,m_{2k+1}) = f_{2k+1}^{(r)} \prod_{i=1}^{k+1} w_{t_i}^{(r)}(m_i) \prod_{i=k+2}^{2k+1} \left[w_{t_i}^{(r)}(m_i)\right]^*, \tag{67}$$

equation (66) can be rewritten as:

$$x_r(n) = \sum_{k=0}^{K} \sum_{t_1=1}^{T} \cdots \sum_{t_{2k+1}=1}^{T} \sum_{m_1=0}^{M} \cdots \sum_{m_{2k+1}=0}^{M} h_{2k+1}^{(r)}(t_1,\ldots,t_{2k+1},m_1,\ldots,m_{2k+1}) \prod_{i=1}^{k+1} s_{t_i}(n-m_i) \prod_{i=k+2}^{2k+1} s_{t_i}^*(n-m_i). \tag{68}$$

From (68) and (67), it can be concluded that a MIMO Wiener system is equivalent to a MIMO Volterra model with separable kernels. Moreover, it should also be highlighted that a MIMO Wiener system can be viewed as convolutive post nonlinear (CPNL) [66] or post nonlinear (PNL) [67, 68] mixtures with polynomial nonlinearities.

4.2 The MIMO Hammerstein model

A SISO Hammerstein system is composed of a memoryless nonlinear block followed by a linear filter, while a MIMO Hammerstein model is composed of memoryless nonlinear blocks in parallel, followed by a linear mixer, as shown in Fig. 2. Note that the Hammerstein system corresponds to the Wiener system with the order of the blocks being inverted.

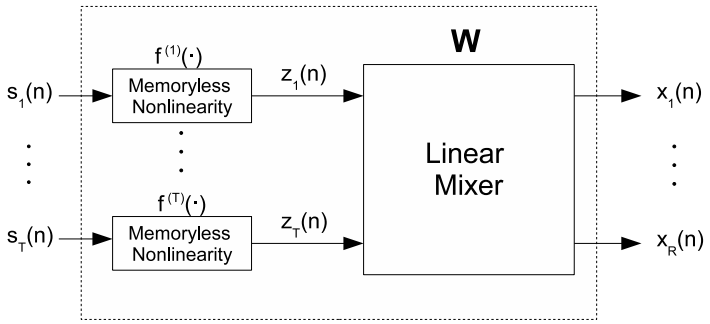

Figure 2: A MIMO Hammerstein system.

Let $z_t(n)$ $(1 \leq t \leq T)$ be the outputs of the memoryless nonlinearities $f^{(t)}(\cdot)$ $(1 \leq t \leq T)$. Using the same assumption about the nonlinear functions as for the Wiener model, we can write:

$$z_t(n) = \sum_{k=0}^{K} f_{2k+1}^{(t)} |s_t(n)|^{2k} s_t(n), \tag{69}$$

where $\{f_1^{(t)}, f_3^{(t)}, \ldots, f_{2K+1}^{(t)}\}$ are the baseband equivalent coefficients of the polynomial function $f^{(t)}(\cdot)$. Denoting by $w_t^{(r)}(m)$ $(0 \leq m \leq M)$ the $(m+1)^{th}$ element of the impulse response associated with the t^{th} input and the r^{th} output, we have:

$$x_r(n) = \sum_{t=1}^{T} \sum_{m=0}^{M} w_t^{(r)}(m) z_t(n-m). \tag{70}$$

Substituting (69) into (70), we get:

$$x_r(n) = \sum_{k=0}^{K} \sum_{t=1}^{T} \sum_{m=0}^{M} f_{2k+1}^{(t)} w_t^{(r)}(m) |s_t(n-m)|^{2k} s_t(n-m). \tag{71}$$

Thus, by defining the following kernel

$$h_{2k+1}^{(r)}(t_1,\ldots,t_{2k+1},m_1,\ldots,m_{2k+1}) = \begin{cases} f_{2k+1}^{(t_1)} w_{t_1}^{(r)}(m_1), & \text{if} \quad t_1 = \ldots = t_{2k+1} \\ & \text{and} \quad m_1 = \ldots = m_{2k+1}, \\ 0, & \text{otherwise}, \end{cases} \tag{72}$$

it is possible to write the output of the MIMO Hammerstein system (71) as the output of the MIMO Volterra model (68). So, it can be concluded that a MIMO Hammerstein system can be viewed as a diagonal MIMO Volterra system.

4.3 The MIMO Wiener-Hammerstein model

A SISO Wiener-Hammerstein system is composed of a static nonlinearity sandwiched between two linear filters, and its MIMO version is composed of static nonlinear blocks in parallel, sandwiched between two linear mixers (see Fig. 3). Note that the Wiener and the Hammerstein models can be viewed as particular cases of a Wiener-Hammerstein system.

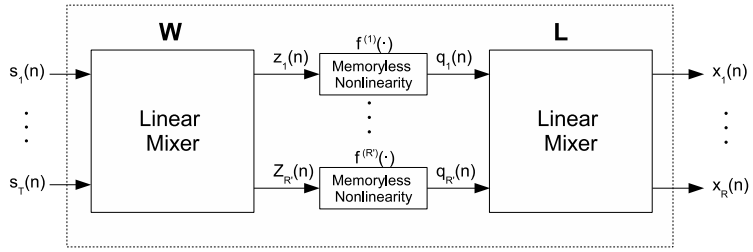

Figure 3: A MIMO Wiener-Hammerstein system.

Let $R^{'}$ be the number of outputs of the first mixer, $z_{r'}(n)$ $(1 \leq r^{'} \leq R^{'})$ the outputs of the first mixer, $q_{r'}(n)$ $(1 \leq r^{'} \leq R^{'})$ the outputs of the nonlinear blocks, $w_t^{(r^{'})}(m)$ $(0 \leq m \leq M_w)$ the $(m+1)^{th}$ element of the impulse response of the first mixer associated with the t^{th} input and the $(r^{'})^{th}$ output, and M_w the memory of the first mixer. From (66), we can write:

$$q_{r'}(n) = \sum_{k=0}^{K} \sum_{t_1=1}^{T} \cdots \sum_{t_{2k+1}=1}^{T} \sum_{m_1=0}^{M_w} \cdots \sum_{m_{2k+1}=0}^{M_w} f_{2k+1}^{(r^{'})} \prod_{i=1}^{k+1} w_{t_i}^{(r^{'})}(m_i) \prod_{i=k+2}^{2k+1} \left[w_{t_i}^{(r^{'})}(m_i) \right]^* \prod_{i=1}^{k+1} s_{t_i}(n-m_i) \prod_{i=k+2}^{2k+1} s_{t_i}^*(n-m_i). \quad (73)$$

On the other hand, the outputs of the MIMO Wiener-Hammerstein system can be expressed as:

$$x_r(n) = \sum_{r'=1}^{R^{'}} \sum_{m=0}^{M_l} l_{r^{'}}^{(r)}(m) q_{r'}(n-m), \quad (74)$$

where $l_{r^{'}}^{(r)}(m)$ $(0 \leq m \leq M_l)$ is the $(m+1)^{th}$ element of the impulse response of the second mixer associated with the $(r^{'})^{th}$ input and the r^{th} output, and M_l is the memory of the second mixer. Substituting (73) into (74), we get:

$$x_r(n) = \sum_{k=0}^{K} \sum_{t_1=1}^{T} \cdots \sum_{t_{2k+1}=1}^{T} \sum_{m_1=0}^{M_w} \cdots \sum_{m_{2k+1}=0}^{M_w} \sum_{r'=1}^{R^{'}} \sum_{m=0}^{M_l} l_{r^{'}}^{(r)}(m) f_{2k+1}^{(r^{'})} \prod_{i=1}^{k+1} w_{t_i}^{(r^{'})}(m_i) \prod_{i=k+2}^{2k+1} \left[w_{t_i}^{(r^{'})}(m_i) \right]^* \prod_{i=1}^{k+1} s_{t_i}(n-m_i-m) \prod_{i=k+2}^{2k+1} s_{t_i}^*(n-m_i-m). \quad (75)$$

By defining:

$$h_{2k+1}^{(r)}(t_1, \ldots, t_{2k+1}, \bar{m}_1, \ldots, \bar{m}_{2k+1}) = \sum_{m=0}^{M_l} \sum_{r'=1}^{R^{'}} l_{r^{'}}^{(r)}(m) f_{2k+1}^{(r^{'})} \left(\prod_{i=1}^{k+1} w_{t_i}^{(r^{'})}(\bar{m}_i - m) \right) \left(\prod_{i=k+2}^{2k+1} \left[w_{t_i}^{(r^{'})}(\bar{m}_i - m) \right]^* \right), \quad (76)$$

with $\bar{m}_{2k+1} = m_{2k+1} + m$, equation (75) can be rewritten as the output of a MIMO Volterra filter:

$$x_r(n) = \sum_{k=0}^{K} \sum_{t_1=1}^{T} \cdots \sum_{t_{2k+1}=1}^{T} \sum_{\bar{m}_1=0}^{M} \cdots \sum_{\bar{m}_{2k+1}=0}^{M} h_{2k+1}^{(r)}(t_1, \ldots, t_{2k+1}, \bar{m}_1, \ldots, \bar{m}_{2k+1}) \prod_{i=1}^{k+1} s_{t_i}(n-\bar{m}_i) \prod_{i=k+2}^{2k+1} s_{t_i}^*(n-\bar{m}_i), \quad (77)$$

where $M = M_w + M_l$.

4.4 Volterra models associated with block-structured nonlinear systems

Note that the MIMO Wiener, Hammerstein and Wiener-Hammerstein models can be viewed as particular cases of MIMO Volterra models. A link between Wiener, Hammerstein and Wiener-Hammerstein models, and the Volterra model was developed in [69] for SISO systems. The above developments linking these MIMO block-structured models with MIMO Volterra models constitute a generalization of the results of [69].

The main advantage of representing Wiener, Hammerstein and Wiener-Hammerstein systems in terms of the parameters of the subsystems, i.e. the linear mixers and memoryless nonlinearities, is that the total number of parameters of these subsystems is, in general, smaller than the number of coefficients of the associated Volterra model. On the other hand, the system output is not linear with respect to the parameters of these subsystems, as we can see in (66), (71) and (75), contrarily to the output of the associated Volterra model. Moreover, a Volterra model allows to take other possible channel nonlinearities into account, contrarily to block-structured models

5. Applications in communication systems

This section is dedicated to some applications of MIMO Volterra models in communication systems, based on the nonlinear MIMO models presented in the previous sections. These applications correspond to situations where the received signals are corrupted by nonlinear ISI, MAI and/or ICI. Applications of Volterra models in other kinds of MIMO communication channels can be found in [20, 30, 36]. In all the following examples, it is assumed perfect symbol synchronization and that the receive filter is matched to the transmit pulse shape filter.

5.1 MIMO channels with nonlinear power amplifiers

In general, all the wireless communication systems employing power amplifiers (PAs) are subject to nonlinear distortions. However, when the signal at the input of the PA is characterized by a high peak-to-average power ratio (PAPR), the introduced nonlinear distortions are particularly important. For these signals, the maximal signal amplitude is high compared to the root mean square (RMS) value. Thus, if the PA operates near the saturation region to obtain a good power efficiency, some components of the input signal fall in the saturation region due to the large fluctuations on the signal envelope. The PA exhibits a nonlinear characteristic at saturation, resulting in the introduction of nonlinear bandlimited distortions. That may lead to significant signal distortion and system performance deterioration.

Some models can be encountered in the literature to represent the nonlinearity of the PA. The Saleh model represents the traveling wave tube (TWT) PA as a frequency independent memoryless nonlinearity characterized by the following amplitude to amplitude (AM/AM) and amplitude to phase (AM/PM) conversions [70]:

$$A(r) = \frac{\alpha_a r}{1 + \beta_a r^2} \tag{78}$$

and

$$\Phi(r) = \frac{\alpha_\phi r^2}{1 + \beta_\phi r^2}, \tag{79}$$

where r is the amplitude of the PA input signal, $A(r)$ and $\Phi(r)$ are respectively the amplitude and phase gains of the PA output signal, and α_a, β_a, α_ϕ and β_ϕ are positive scalar constants.

Radio frequency PAs can also be modeled using polynomial models such as Volterra models. The simplest polynomial model for a PA is given by the following equivalent baseband input-output relationship [17, 71, 72]:

$$x(n) = \sum_{k=0}^{K} f_{2k+1} \left|s(n)\right|^{2k} s(n). \tag{80}$$

If the polynomial coefficients f_{2k+1} are real-valued, the model (80) is strictly memoryless, which means that the PA introduces only amplitude distortion (AM/AM conversion). However, if the coefficients f_{2k+1} are complex-valued, the model (80) allows representing a more general class of models called quasi-memoryless PA [71–73]. In this case, if the memory of the PA is short compared to the time variations of the input signal envelope, equation (80) may represent the output of a PA with amplitude and phase distortions (AM/AM and AM/PM conversions).

Nevertheless, when the bandwidth of the input signal is large, in general, the memory of the PA can not be considered short with respect to the time variations of the input signal [17, 71]. More complex models must then be used to take the memory effects of the PA into account. In this case, among the nonlinear models usually considered in the literature for modeling the PA, the most general is given by the SISO Volterra model (40) [71, 72, 74]. Several special cases of the Volterra model can also be used for modeling the PA nonlinearities as SISO Wiener, Hammerstein and Wiener-Hammerstein models [71, 72, 75]. Moreover, PAs with memory effects are also often modeled as a diagonal Volterra model [22, 71, 72, 74, 76–78]:

$$x(n) = \sum_{k=0}^{K} \sum_{m=0}^{M} f_{2k+1}(m) \left|s(n-m)\right|^{2k} s(n-m). \tag{81}$$

This model is also referred to as memory polynomial model and can be viewed as a generalization of the SISO Hammerstein model. For further details about the PA models, see [70, 79] and references therein. In the sequel, two kinds of wireless communication systems that can be modeled as MIMO Volterra models are presented.

5.1.1 OFDM systems

Orthogonal frequency division multiplexing (OFDM) signals are especially vulnerable to PA nonlinear distortions due to their high peak-to-average power ratio (PAPR) [18–24], caused by the sum of several symbols with different phases and frequencies. The PAPR of a signal is defined as the ratio of its maximum squared amplitude to the average power [80]. This means that, if the PAPR of a signal is high, the maximal signal power is high compared to the average signal power, i.e. the signal has large envelope fluctuations. As a consequence, the received signals in a OFDM system are particularly affected by the presence of a nonlinear PA. In this case, a nonlinear PA results in the introduction of nonlinear ICI between the subcarriers. Theoretical analysis and performance of OFDM signals in nonlinear channels have been widely studied in the literature [22–24, 81–83]. In this case, a single-user channel can be modeled as a cascade of a nonlinear system, corresponding to the PA, followed by a linear filter corresponding to the frequency selective fading wireless link. The global channel (PA + wireless link) can then be modeled as a Volterra system [19].

MIMO transmission schemes can be used in OFDM systems to provide an efficient radio spectrum, allowing a good reuse of the same frequency range to increase the data rate and the system capacity. In this case, the global channel between each source (Tx antenna or user) and each receive antenna can be modeled as Volterra system and the global MIMO-OFDM channel can be expressed as the MIMO Volterra model (49). Note that, due to the fact that the nonlinearity is at the transmitter, the nonlinear MIMO-OFDM channel does not contain products of different sources. The signal of each source, corrupted by nonlinear ICI, is linearly mixed with the signal of the other sources. In this case, the global MIMO-OFDM channel can also be modeled as a MIMO Hammerstein system. Using the notation introduced in Section 4.1, we have:

- $f_{2k+1}^{(t)}$ denotes coefficients of the polynomial function representing the PA of the t^{th} antenna element.
- $w_t^{(r)}(m), m = 0, 1, ...M$, denotes the channel impulse response of the wireless channel between the t^{th} user and the r^{th} receive antenna.

However, it should be highlighted that the OFDM technology allows a great simplification in the modeling of MIMO Volterra channels [84].

5.1.2 Satellite systems

In satellite communication systems, the signals are transmitted from a ground (earth) station towards a satellite station (uplink) and then retransmitted to a receive ground station (downlink). Due to power limitation, the satellite station usually employs a PA [15], often in the form of a TWT or a solid-state power amplifier (SSPA), that is driven at or near saturation in order to obtain a power efficient transmission [10, 13, 14, 16], resulting in the introduction of nonlinear distortions.

The overall satellite channel, i.e. the cascade of the uplink, PA and downlink, was first modeled as an equivalent baseband SISO Volterra system by Benedetto *et al*. [9], its effectiveness for modeling this kind of channels being verified in [10]. In some cases, the Volterra model for the satellite channel incorporates the satellite pre- and post-filters [10, 50–52]. Satellite channels can also be modeled as a SISO Wiener-Hammerstein system, the wireless uplink and downlink being represented by linear filters and the PA by a memoryless polynomial model [10, 79].

In order to improve the transmission spectral efficiency, the use of MIMO satellite systems has been considered in several works [85–89]. Concerning the structure of the MIMO satellite link, the following configuration is usually considered: the ground station with multiple transmit antennas transmits towards multiple satellites with a single antenna each one, that retransmits towards another ground station with multiple receive antennas. We can also consider the case where the T sources correspond to various ground stations with a single transmit antenna, i.e. mobile unites transmitting towards a single receive station. In these cases, the channel can be represented by a MIMO Wiener-Hammerstein model, with:

- the wireless uplink being modeled as a linear $T \times R^{'}$ mixer with channel impulse responses denoted by $w_t^{(r^{'})}(m), m = 0, 1, ...M_w, t = 1, ..., T, r^{'} = 1, ..., R^{'}$;
- $f_{2k+1}^{(r^{'})}$ denoting coefficients of the polynomial function representing the PA, $r^{'} = 1, ..., R^{'}$.
- the wireless downlink being modeled as a linear $R^{'} \times R$ mixer with impulse responses denoted by $l_{r^{'}}^{(r)}(m), m = 0, 1, ...M_w, r = 1, ..., R, r^{'} = 1, ..., R^{'}$.

The wireless link of the satellite channel has often a line-of-sight propagation [90] and the satellite channel delay spread is usually small [10]. In fact, some authors assume that the transmitted signals are narrowband with respect to the channel's coherence bandwidth [90, 91], i.e. the wireless channel has a flat fading.

5.2 Radio Over Fiber (ROF) channels

ROF links have found a new important application with their introduction in micro- and pico-cellular wireless networks [25, 26, 40, 92, 93]. Micro- and pico-cellular architectures provide to the system a better capacity, coverage and power consumption, especially in hot-spot areas. Thus, they can also improve the system reliability and Quality of Service. ROF links provide a cost-effective solution for important problems like station complexity and bandwidth limitation [94]. In ROF systems, the uplink transmission is done from a mobile station towards radio access points, which are merely low-cost remote antenna stations consisting of an electro-optical converter and a transponder [95]. At the radio access points, the transmitted signals are converted in optical frequencies by a laser diode and then retransmitted through optical fibers towards a central base station, as summarized in Fig. 4. Most part of the signal processing, such as channel estimation, equalization, modulation and demodulation, is done at the central base station [25, 26, 95].

Important nonlinear distortions are introduced by the laser diode at the electrical-optical (E/O) conversion device [25–27, 40, 92]. Gain compression characteristics combined with stimulated and spontaneous mechanisms of emission make the laser inherently nonlinear [25]. Other phenomena, as leakage current and "axial hole burning" may also be sources of nonlinearities [25]. The E/O nonlinearity in a ROF system is often modeled using a memoryless polynomial model [25–27, 40]. For more details about the ROF nonlinearities, see [25] and references therein.

Concerning the optical link, chromatic dispersion is some of the main concerns with single-mode and multi-mode fibers. The transfer function of a fiber reflecting the chromatic dispersion, is given by [25]:

$$H(f) = e^{-\mathbf{j}\alpha l(f-f_o)^2} \tag{82}$$

where α is a dispersion coefficient, l is the fiber length and f_o is the optical carrier frequency. For a wavelength of 1310 nm, the chromatic dispersion of the fiber is not significant up to several hundreds of kilometers of fiber length and up to few GHz [25, 92, 96]. This means that the chromatic dispersion of the fiber is negligible and the nonlinear distortion arising from the E/O conversion process becomes then preponderant. Thus, the overall uplink channel can be viewed as a wireless link followed by an E/O conversion. In a single-user and a single receive antenna case, the wireless link can be modeled as a linear filter and the overall ROF uplink channel as a SISO Wiener model [25, 27, 92] .

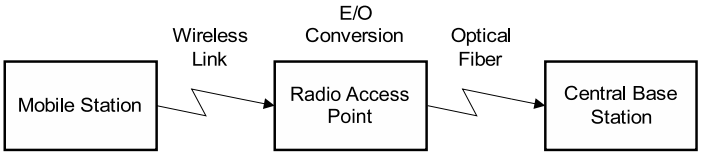

Figure 4: Radio-over-fiber uplink diagram.

Aiming to supply the growing demand for system capacity, technologies such as smart antennas (or MIMO) and ROF transmission can be used together [94, 97]. In a ROF system with an antenna array at the radio access point, the optical link between the antenna array and the central base station can be implemented using either multiple fibers or a single fiber with wavelength division multiplexing (WDM) [94, 95, 97]. The second case is particularly interesting, as the use of an antenna array can be done using the same optical components already installed for the ROF system [97]. In this case, the signal received at the radio access point is multiplexed, a single optical carrier being assigned to each antenna element, and then transmitted over the optical fiber, followed by an optical carrier demultiplexing.

In a multiuser channel employing an antenna array at the radio access point, the wireless link can be modeled as a linear mixture and the overall ROF uplink as a MIMO Wiener model. In this case, using the notation introduced in Section 4.1, we have:

- $w_t^{(r)}(m), m = 0, 1, ...M$, denotes the channel impulse response of the wireless channel between the $t^{\,th}$ user and the r^{th} receive antenna;
- $f_{2k+1}^{(r)}$ denotes coefficients of the polynomial function representing the nonlinear E/O conversion device associated with the r^{th} antenna element.

Thus, using the developments of Section 4.1, the ROF uplink channel can be modeled as a MIMO Volterra filter like (68). Besides, ROF links have been considered in the context of CDMA systems [27, 40, 93, 98], as well as for OFDM 802.11a systems [93–95, 99].

The downlink channel of a ROF can be modeled similarly as the uplink. However, in this case, the wireless channel is placed after the E/O conversion [25]. The overall channel can then be viewed as a Hammerstein system. Besides, at the downlink, the received signals are more subject to nonlinear distortions due to PA saturation than at the uplink.

6. Conclusion

An overview of nonlinear communication channels using MIMO Volterra models has been presented in this paper. These models are very useful for modelling a large class of nonlinear systems. Starting from the standard continuous-time SISO Volterra channel, the equivalent baseband discrete-time SISO Volterra channel has been established, with its triangular and vectorial forms. Besides, the Fourier transform of the equivalent baseband discrete-time SISO Volterra channel output has been derived, which allowed us to explain the spectral broadening produced by a Volterra system. Based on the SISO Volterra channel representation, we developed the expression of an equivalent baseband discrete-time MIMO Volterra model that does not contain products of different sources. Then, we developed the MIMO Volterra model that allows to represent a nonlinear mixture of sources, and finally, we presented the MIMO Volterra model characterized by different memories with respect to the inputs, as well as its triangular and vector forms.

The developments carried out in this paper are of great importance due to the lack of works dealing with nonlinear MIMO communication channels. Moreover, it contains two original contributions. The first one is the development of the general expressions for equivalent baseband discrete-time MIMO Volterra channels and the second one is the development of the relationships between MIMO Volterra and MIMO Wiener, Hammerstein and Wiener-Hammerstein models. It was demonstrated that MIMO Wiener, Hammerstein and Wiener-Hammerstein models can be viewed as special cases of MIMO Volterra models. Moreover, three applications of MIMO Volterra models for OFDM, satellite and ROF communication systems have been briefly described.

Appendix: The truncated Kronecker product

The *truncated Kronecker product* of the vector $\mathbf{a} \in \mathbb{C}^{L\times 1}$ by itself is defined in the following way:

$$\oslash^2\mathbf{a} = \mathbf{a} \oslash \mathbf{a} = \begin{pmatrix} a_1\bar{\mathbf{a}}_1 \\ a_2\bar{\mathbf{a}}_2 \\ \vdots \\ a_{L-1}\bar{\mathbf{a}}_{L-1} \\ a_L^2 \end{pmatrix} \in \mathbb{C}^{\frac{L(L+1)}{2}\times 1}, \tag{83}$$

where $\bar{\mathbf{a}}_i = [a_i\ a_{i+1} \dots a_L]^T \in \mathbb{C}^{(L-i+1)\times 1}$. The truncated Kronecker product does not include the redundant terms that are present in the Kronecker product of a vector by itself, which means that the vector $\oslash^2\mathbf{a}$ does not contain repeated components. It is also possible to define the N^{th}-order power of the truncated Kronecker product of a vector $\mathbf{a}$, denoted $\oslash^N\mathbf{a} = \mathbf{a} \oslash \cdots \oslash \mathbf{a}$ ($N-1$ times the operator $\oslash$), by means of the following recursion:

$$\oslash^N\mathbf{a} = \begin{pmatrix} a_1 \oslash^{N-1} \bar{\mathbf{a}}_1 \\ a_2 \oslash^{N-1} \bar{\mathbf{a}}_2 \\ \vdots \\ a_{L-1} \oslash^{N-1} \bar{\mathbf{a}}_{L-1} \\ a_L^N \end{pmatrix}, \tag{84}$$

with $\oslash^1\mathbf{a} = \mathbf{a}$. The vector $\oslash^N\mathbf{a}$ contains all the N^{th}-order products of the elements of $\mathbf{a}$, with no repeated terms. The dimension of the vector $\oslash^N\mathbf{a}$ is given by the number of subsets of cardinality N with elements taken from a set of cardinality L, i.e. the number of combinations with repetition of N elements drawn from a set of cardinality L:

$$C_{L,N} = \frac{(L+N-1)!}{(L-1)!N!}. \tag{85}$$

REFERENCES

[1] V. Volterra. *Theory of Functionals and of Integral and Integro-Differential Equations*. New York: Dover Publications, 1959.

[2] M. Schetzen. *The Volterra and Wiener theories of nonlinear systems*. John Wiley and Sons, Inc., New-York, USA, 1980.

[3] N. Wiener. *Nonlinear Problems in Random Theory*. MIT Press, Cambridge, MA, USA, 1958.

[4] P. Z. Marmarelis and V. Z. Marmarelis. *Analysis of Physiological Systems*. Plenum, New-York, USA, 1978.

[5] M. J. Korenberg and I. W. Hunter. "The identification of nonlinear biological systems: LNL cascade models". *Biological Cybernetics*, vol. 55, no. 2–3, pp. 125–134, Nov. 1986.

[6] G. B. Giannakis and E. Serpedin. "A bibliography on nonlinear system identification". *Signal Processing*, vol. 81, no. 3, pp. 533–580, Mar. 2001.

[7] E. Biglieri, E. Chiaberto, G. P. Maccone and E. Viterbo. "Compensation of nonlinearities in high-density magnetic recording channels". *IEEE Transactions on Magnetics*, vol. 30, no. 6, pp. 5079–5086, Nov. 1994.

[8] J. C. Ralston and A. M. Zoubir. "Identification of a class of multiple input–output nonlinear systems driven by stationary non-Gaussian processes". In *IEEE Signal Processing Workshop on Statistical Signal and Array Processing*, pp. 379–382, Corfu, Greece, Jun. 1996.

[9] S. Benedetto, E. Biglieri and R. Daffara. "Modeling and performance evaluation of nonlinear satellite links - A Volterra series approach". *IEEE Transactions on Aerospace Electronic Systems*, vol. 15, pp. 494–507, Jul. 1979.

[10] S. Benedetto and E. Biglieri. "Nonlinear Equalization of Digital Satellite Channels". *IEEE Journal on Selected Areas in Communications*, vol. 1, no. 1, pp. 57–62, Jan. 1983.

[11] E. Biglieri, A. Gersho, R. Gitlin and T. Lim. "Adaptive cancellation of nonlinear intersymbol interference for voiceband data transmission". *IEEE Journal on Selected Areas in Communications*, vol. 2, no. 5, pp. 765–777, 1984.

[12] S. Benedetto, E. Biglieri and V. Castellani. *Digital Transmission Theory*. Prentice-Hall, 1987.

[13] I.-K. Hwang and L. Kurz. "Digital data transmission over nonlinear satellite channels". *IEEE Transactions on Communications*, vol. 41, no. 11, pp. 1694–1702, Nov. 1993.

[14] A. Uncini, L. Vecci, P. Campolucci and F. Piazza. "Complex-Valued Neural Networks with Adaptive Spline Activation Function for Digital Radio Links Nonlinear Equalization". *IEEE Transactions on Signal Processing*, vol. 47, no. 2, pp. 505–514, Feb. 1999.

[15] S. C. Cripps. *RF Power Amplifiers for Wireless Communications*. Artech House, 1999.

[16] A. Gutierrez and W. E. Ryan. "Performance of Volterra and MLSD Receivers for Nonlinear Band-Limited Satellite Systems". *IEEE Transactions on Communications*, vol. 48, no. 7, pp. 1171–1177, Jul. 2000.

[17] G. Zhou and R. Raich. "Spectral analysis of polynomial nonlinearity with applications to RF power amplifiers". *EURASIP Journal on Applied Signal Processing*, vol. 12, pp. 1831–1840, 2004.

[18] A. N. D'Andrea, V. Lottici and R. Reggiannini. "Nonlinear predistortion of OFDM signals over frequency-selective fading channels". *IEEE Transactions on Communications*, vol. 49, no. 5, pp. 837–843, May 2001.

[19] A. J. Redfern and G. T. Zhou. "Nonlinear channel identification and equalization for OFDM systems". In *IEEE International Conference on Acoustics, Speech and Signal Processing (ICASSP)*, volume 6, pp. 3521–3524, Seattle, WA,USA, May 1998.

[20] A. I. Sulyman and M. Ibnkahla. "Performance analysis of non-linearly amplified M-QAM signals in MIMO channels". In *IEEE International Conference on Acoustics, Speech and Signal Processing (ICASSP)*, volume 4, pp. iv–401–iv–404, Montreal, Canada, May 2004.

[21] C. Xia and J. Ilow. "Blind Compensation of Memoryless Nonlinear Effects in OFDM Transmissions Using CDF". In *Communication Networks and Services Research Conference*, Moncton, Canada, May 2003.

[22] V. A. Bohara and S. H. Ting. "Analysis of OFDM Signals in Nonlinear High Power Amplifier with Memory". In *IEEE International Conference on Communications*, pp. 3653–3657, Beijing, China, May 2008.

[23] P. Banelli and S. Cacopardi. "Theoretical Analysis and Performance of OFDM Signals in Nonlinear AWGN Channels". *IEEE Transactions on Communications*, vol. 48, no. 3, pp. 430–441, Mar. 2000.

[24] P. Banelli, G. Baruffa and S. Cacopardi. "Effects of HPA Nonlinearity on Frequency Multiplexed OFDM Signals". *IEEE Transactions on Broadcasting*, vol. 47, no. 2, pp. 123–136, Jun. 2001.

[25] X. N. Fernando and A. B. Sesay. "Adaptive asymmetric linearization of radio over fiber links for wireless access". *IEEE Transactions on Vehicular Technology*, vol. 51, no. 6, pp. 1576–1586, Nov. 2002.

[26] X. N. Fernando and A. B. Sesay. "A Hammerstein-Type Equalizer for Concatenated Fiber-Wireless Uplink". *IEEE Transactions on Vehicular Technology*, vol. 54, no. 6, pp. 1980–1991, 2005.

[27] S. Z. Pinter and X. N. Fernando. "Estimation of radio-over-fiber uplink in a multiuser CDMA environment using PN spreading codes". In *Canadian Conference on Electrical and Computer Engineering*, pp. 1–4, Saskatoon, Canada, May 2005.

[28] S. Z. Pinter and X. N. Fernando. "Equalization of Multiuser Wireless CDMA Downlink Considering Transmitter Nonlinearity Using Walsh Codes". *EURASIP Journal on Wireless Communications and Networking*, vol. 2007, no. 1, Jan. 2007.

[29] K. Witrisal, G. Leus, M. Pausini and C. Krall. "Equivalent System Model and Equalization of Differential Impulse Radio UWB Systems". *IEEE Journal on Selected Areas in Communications*, vol. 23, no. 9, pp. 1851–1862, Sep. 2005.

[30] N. Petrochilos and K. Witrisal. "Semi-Blind Source Separation for Memoryless Volterra Channels in UWB and its Uniqueness". In *IEEE Workshop on Sensor Array and Multichannel Processing*, pp. 566–570, Waltham, MA, USA, Jul. 2006.

[31] K. Shi, X. Ma and G. T. Zhou. "A residual echo suppression technique for systems with nonlinear acoustic echo paths". In *IEEE International Conference on Acoustics, Speech, and Signal Processing (ICASSP)*, pp. 257–260, Las Vegas, NV, USA, Apr. 2008.

[32] K. Shi, X. Ma and G. T. Zhou. "Adaptive acoustic echo cancellation in the presence of multiple nonlinearities". In *IEEE International Conference on Acoustics, Speech, and Signal Processing (ICASSP)*, volume 2, pp. 3601–3604, Las Vegas, NV, USA, Apr. 2008.

[33] D. A. Bendersky, J. W. Stokes and H. S. Malvar. "Nonlinear residual acoustic echo suppression for high levels of harmonic distortion". In *IEEE International Conference on Acoustics, Speech, and Signal Processing (ICASSP)*, volume 2, pp. 261–264, Las Vegas, NV, USA, Apr. 2008.

[34] Q. Zou, M. Mikhemar and A. H. Sayed. "Digital compensation of RF nonlinearities in software-defined radios". In *IEEE International Conference on Acoustics, Speech and Signal Processing (ICASSP)*, pp. 2921–2924, Las Vegas, NV,USA, Apr. 2008.

[35] S.-W. Chen, W. Panton and R. Gilmore. "Effects of nonlinear distortion on CDMA communication systems". *IEEE Transactions on Microwave Theory and Techniques*, vol. 44, no. 12, pp. 2743–2750, Dec. 1996.

[36] A. J. Redfern and G. T. Zhou. "Blind zero forcing equalization of multichannel nonlinear CDMA systems". *IEEE Transactions on Signal Processing*, vol. 49, no. 10, pp. 2363–2371, Oct. 2001.

[37] A. Conti, D. Dardari and V. Tralli. "An Analytical Framework for CDMA systems with a Nonlinear Amplifier and AWGN". *IEEE Transactions on Communications*, vol. 50, no. 7, pp. 1110–1120, Jul. 2002.

[38] F. Gregorio, S. Werner, T. I. Laakso and J. Cousseau. "Receiver Cancellation Technique for Nonlinear Power Amplifier Distortion in SDMA-OFDM Systems". *IEEE Transactions on Vehicular Technology*, vol. 56, no. 5, pp. 2499–2516, Sep. 2007.

[39] T. C. W. Schenk, C. Dehos, D. Morche and E. R. Fledderus. "Receiver-Based Compensation of Transmitter-Incurred Nonlinear Distortion in Multiple-Antenna OFDM Systems". In *IEEE Vehicular Technology Conference - Fall*, pp. 1346–1350, Baltimore, MD, USA, Oct. 2007.

[40] S. Z. Pinter and X. N. Fernando. "Concatenated fiber-wireless channel identification in a multiuser CDMA environment". *IET Communications*, vol. 1, no. 5, pp. 937–944, Oct. 2007.

[41] C. K. An, E. J.Powers and C. P. Ritz. "Frequency domain modeling of dual–input/multiple–output quadratic systems with general random inputs". In *IEEE International Symposium on Circuits and Systems*, volume 3, pp. 2209–2212, Monterey, CA, USA, Jun. 1998.

[42] C. Seretis and E. Zafiriou. "Nonlinear dynamical system identification using reduced Volterra models with generalized orthonormal basis functions". In *American Control Conference*, volume 5, pp. 3042–3046, Albuquerque, NM, USA, Jun. 1997.

[43] K. D. Rao and D. C. Reddy. "Design of Multi-Input Multi-Output Adaptive Volterra Filters". In *Digital Signal Processing Workshop*, pp. 8.11.1–8.11.2, Sep. 1992.

[44] G. B. Giannakis and E. Serpedin. "Linear Multichannel Blind Equalizers of Nonlinear FIR Volterra channels". *IEEE Transactions on Signal Processing*, vol. 45, no. 1, pp. 67–81, Jan. 1997.

[45] J. Fang, A. R. Leyman, Y. H. Chew and H. Duan. "Some further results on blind identification of MIMO FIR channels via second-order statistics". *Signal Processing*, vol. 87, no. 6, pp. 1434–1447, Jun. 2007.

[46] R. Lopez-Valcarce and S. Dasgupta. "Blind Equalization of Nonlinear Channels From Second-Order Statistics". *IEEE Transactions on Signal Processing*, vol. 49, no. 12, pp. 3084–3097, Dec. 2001.

[47] S. Boyd and L. O. Chua. "Fading memory and the problem of approximating nonlinear operators with Volterra series". *IEEE Transactions on Circuits and Systems*, vol. 32, no. 11, pp. 1150–1161, Nov. 1985.

[48] D. Hummels and R. Gitchell. "Equivalent Low-Pass Representations for Bandpass Volterra Systems". *IEEE Transactions on Communications*, vol. 28, no. 1, pp. 140–142, Jan. 1980.

[49] E. Aschbacher. "Digital Pre-distortion of Microwave Power Amplifiers". Ph.D. thesis, Vienna University of Technology, Austria, Sep. 2005.

[50] E. Biglieri. "High-Level Modulation and Coding for Nonlinear Satellite Channels". *IEEE Transactions on Communications*, vol. 32, no. 5, pp. 616–626, May 1984.

[51] A. Gutierrez and W. E. Ryan. "Performance of Adaptive Volterra Equalizers on Nonlinear Satellite Channels". In *IEEE International Conference on Communications*, volume 1, pp. 488–492, Seattle, WA, USA, Jun. 1995.

[52] Y. T. Su, M.-C. Chiu and Y.-C. Chen. "Turbo Equalization of Nonlinear TDMA Satellite Signals". In *IEEE Global Telecommunications Conference*, volume 3, pp. 2860–2864, Taipei, Taiwan, Nov. 2002.

[53] J. Tsimbinos and K. V. Lever. "Input Nyquist Sampling Suffices to Identify and Compensate Nonlinear Systems". *IEEE Transactions on Signal Processing*, vol. 46, no. 10, pp. 2833–2837, Oct. 1998.

[54] R. J. Martin. "Volterra system identification and Kramer's sampling theorem". *IEEE Transactions on Signal Processing*, vol. 47, no. 11, pp. 3152–3155, Nov. 1999.

[55] A. V. Oppenheim, R. W. Schafer and J. R. Buck. *Discrete-Time Signal Processing*. Prentice-Hall, second edition, 1998.

[56] R. Lopez-Valcarce and S. Dasgupta. "Second-order statistical properties of nonlinearly distorted phase-shift keyed (PSK) signals". *IEEE Communications Letters*, vol. 7, no. 7, pp. 323–325, Jul. 2003.

[57] C. A. R. Fernandes, G. Favier and J. C. M. Mota. "Blind Source Separation and Identification of Nonlinear Multiuser Channels using Second Order Statistics and Modulation Codes". In *IEEE International Workshop Signal Processing Advances in Wireless Communications (SPAWC)*, Helsinki, Finland, Jun. 2007.

[58] C. A. R. Fernandes, G. Favier and J. C. M. Mota. "Blind Tensor-Based Identification of Memoryless Multiuser Volterra Channels Using SOS and Modulation Codes". In *European Signal Processing Conference (EUSIPCO)*, Poznan, Poland, Sep. 2007.

[59] C. A. R. Fernandes, G. Favier and J. C. M. Mota. "A Modulation Code-Based Blind Receiver for Memoryless Multiuser Volterra Channels". In *ASILOMAR Conference on Siginal, Systems, and Computers*, Pacific Grove, CA, USA, Nov. 2007.

[60] C. A. R. Fernandes, G. Favier and J. C. M. Mota. "Blind Estimation of Nonlinear Instantaneous Channels in Multiuser CDMA systems with PSK inputs". In *IEEE International Workshop Signal Processing Advances in Wireless Communications (SPAWC)*, Recife, Brazil, Jul. 2008.

[61] C. A. R. Fernandes, G. Favier and J. C. M. Mota. "Tensor Based Receivers for Nonlinear Radio Over Fiber Uplinks in Multiuser CDMA Systems". In *IEEE International Symposium on Personal, Indoor and Mobile Radio Communications (PIMRC)*, Cannes, France, Sep. 2008.

[62] C. A. R. Fernandes, G. Favier and J. C. M. Mota. "Blind Identification of Multiuser Nonlinear Channels Using Tensor Decomposition and Precoding". *Signal Processing,*, vol. 89, no. 12, pp. 2644–2656, Dec. 2009.

[63] C. A. R. Fernandes, G. Favier and J. C. M. Mota. "Tensor-Based Blind Identification of MIMO Volterra Channels in a Multiuser CDMA Environment". In *European Signal Processing Conference (EUSIPCO)*, Lausanne , Switzerland, Aug. 2008.

[64] C. A. R. Fernandes, G. Favier and J. C. M. Mota. "Input Orthogonalization Methods for Third-Order MIMO Volterra Channel Identification". In *Colloque GRETSI*, Troyes, France, Sep. 2007.

[65] W. Greblicki. "Nonparametric identification of Wiener systems by orthogonal series". *IEEE Transactions on Automatic Control*, vol. 39, no. 10, pp. 2077–2086, Oct. 1994.

[66] M. Babaie-Zadeh, C. Jutten and K. Nayebi. "Separating convolutive post non-linear mixtures". In *Workshop on Independent Component Analysis and Signal Separation*, pp. 138–143, San Diego, CA, USA, 2001.

[67] A. Taleb and C. Jutten. "Source separation in post-nonlinear mixtures". *IEEE Transactions on Signal Processing*, vol. 47, no. 10, pp. 2807–2820, Sep. 1999.

[68] C. Jutten, M. Babaie-Zadeh and S. Hosseini. "Three easy ways for separating nonlinear mixtures?" *Signal Processing*, vol. 84, no. 2, pp. 217–229, Feb. 2004.

[69] A. Y. Kibangou and G. Favier. "Wiener-Hammerstein systems modeling using diagonal Volterra kernels coefficients". *IEEE Signal Processing Letters*, vol. 13, no. 6, pp. 381–384, Jun. 2006.

[70] A. A. M. Saleh. "Frequency-independent and frequency dependent nonlinear models of TWT amplifiers". *IEEE Transactions on Communications*, vol. COM-29, pp. 1715–1720, Nov. 1981.

[71] L. Ding. "Digital Predistortion of Power Amplifiers for Wireless Applications". Ph.D. thesis, School of Electrical and Computer Engineering, Georgia Institute of Technology, USA, Mar. 2004.

[72] R. Raich. "Nonlinear System Identification and Analysis with Applications to Power Amplifier Modeling and Power Amplifier Predistortion". Ph.D. thesis, School of Electrical and Computer Engineering, Georgia Institute of Technology, USA, Mar. 2004.

[73] R. Raich and G. T. Zhou. "On the modeling of memory nonlinear effects of power amplifiers for communication applications". In *IEEE Digital Signal Processing Workshop*, pp. 7–10, Pine Mountain, GA, USA, Oct. 2002.

[74] L. Ding, G. T. Zhou, D. R. Morgan, Z. Ma, J. S. Kenney, J. Kim and C. R. Giardina. "A Robust Digital Baseband Predistorter Constructed Using Memory Polynomials". *IEEE Transactions on Communications*, vol. 52, no. 1, pp. 159–165, Jan. 2004.

[75] C. J. Clark, G. Chrisikos, M. S. Muha, A. A. Moulthrop and C. P. Silva. "Time domain envelope measurement technique with application to wideband power amplifier modeling". *IEEE Transactions on Microwave theory and techniques*, vol. 46, no. 12, pp. 2531–2540, Dec. 1998.

[76] R. Marsalek. "Contributions to the power amplifier linearization using digital baseband adaptive predistortion". Ph.D. thesis, Université de Marne-la-Vallée, France, 2003.

[77] F. Gregorio. "Analysis and compensation of nonlinear power amplifiers effects in multi-antenna OFDM systems". Ph.D. thesis, Helsinki University of Technology, Finland, 2007.

[78] Y. Ding and A. Sano. "Time-domain adaptive predistortion for nonlinear amplifiers". In *IEEE International Conference on Acoustics, Speech and Signal Processing (ICASSP)*, volume 2, pp. ii–865–ii–868, Montreal, Canada, May 2004.

[79] M. Ibnkahla, N. J. Bershad, J. Sombrin and F. Castanie. "Neural network modeling and identification of nonlinear channels with memory: algorithms, applications, and analytic models". *IEEE Transactions on Communications*, vol. 46, no. 5, pp. 1208–1220, May 1998.

[80] S. Litsyn. *Peak Power Control in Multicarrier Communications*. Cambridge University Press, first edition, 2007.

[81] E. Costa and S. Pupolin. "M-QAM-OFDM System Performance in the Presence of a Nonlinear Amplifier and Phase Noise". *IEEE Transactions on Communications*, vol. 50, no. 3, pp. 462–472, Mar. 2002.

[82] D. Dardari, V. Tralli and A. Vaccari. "A Theoretical Characterization of Nonlinear Distortion Effects in OFDM Systems". *IEEE Transactions on Communications*, vol. 48, no. 10, pp. 1755–1764, Oct. 2000.

[83] V. A. Bohara and S. H. Ting. "Theoretical analysis of OFDM signals in nonlinear polynomial models". In *International Conference on Information, Communications and Signal Processing*, pp. 10–13, Singapore City, Singapore, Dec. 2007.

[84] C. A. R. Fernandes. "Nonlinear MIMO Communication Systems: Channel Estimation and Information Recovery using Volterra Models". Ph.D. thesis, University of Nice - Sophia Antipolis, France & Federal University of Ceará, Brazil, Jul. 2009.

[85] R. T. Schwarz, A. Knopp, D. Ogermann, C. A. Hofinann and B. Lankl. "Optimum-capacity MIMO satellite link for fixed and mobile services". In *International ITG Workshop on Smart Antennas*, pp. 209–216, Darmstadt, Germany, Feb. 2008.

[86] P. R. King and S. Stavrou. "Capacity Improvement for a Land Mobile Single Satellite MIMO System". *IEEE Antennas and Wireless Propagation Letters*, vol. 5, no. 1, pp. 98–100, Dec. 2006.

[87] P. R. King and S. Stavrou. "Characteristics of the Land Mobile Satellite MIMO Channel". In *IEEE Vehicular Technology Conference - Fall*, pp. 1–4, Montreal, Canada, Sep. 2006.

[88] P. R. King and S. Stavrou. "Low Elevation Wideband Land Mobile Satellite MIMO Channel Characteristics". *IEEE Transactions on Wireless Communications*, vol. 6, no. 7, pp. 2712–2720, Jul. 2007.

[89] F. Yamashita, K. Kobayashi, M. Ueba and M. Umehira. "Broadband multiple satellite MIMO system". In *IEEE Vehicular Technology Conference - Fall*, volume 4, pp. 2632–2636, Dallas, TX, USA, Sep. 2005.

[90] C. Dubuc, D. Boudreau and F. Patenaude. "The Design and Simulated Performance of a Mobile Video Telephony Application for Satellite Third-Generation Wireless Systems". *IEEE Transactions on Multimedia*, vol. 3, no. 4, pp. 424–431, Dec. 2001.

[91] S. D. Silverstein. "Application of Orthogonal Codes to the Calibration of Active Phased Array Antennas for Communication Satellites". *IEEE Transactions on Signal Processing*, vol. 45, no. 1, pp. 206–218, Jan. 1997.

[92] X. N. Fernando and A. B. Sesay. "Higher order adaptive filter based predistortion for nonlinear distortion compensation of radio over fiber links". In *IEEE International Conference on Communications*, volume 1/3, pp. 367–371, New-Orleans, LA, USA, Jun. 2000.

[93] S. Z. Pinter and X. N. Fernando. "Fiber-Wireless Solution for Broadband Multimedia Access". *IEEE Canadian Review - Summer*, , no. 50, pp. 6–9, 2005.

[94] Y. Kim, S. Doucet, M. E. M. Pasandi and S. LaRochelle. "Optical multicarrier generator for radio-over-fiber systems". *Optics Express*, vol. 16, no. 2, pp. 1068–1076, Jan. 2008.

[95] M. Sauer, A. Kobyakov and J. George. "Radio Over Fiber for Picocellular Network Architectures". *Journal of Lightwave Technology*, vol. 25, no. 11, pp. 3301–3320, Nov. 2007.

[96] W. Way. "Optical fiber based microcellular systems. An overview". *IEICE Transactions on Communications*, vol. E76-B, no. 9, pp. 1091–1102, Sep. 1993.

[97] P. Ritosa, B. Batagelj and M. Vidmar. "Optically steerable antenna array for radio over fibre transmission". *Electronics Letters*, vol. 41, no. 16, pp. 47–48, Aug. 2005.

[98] X. N. Fernando and A. B. Sesay. "Characteristics of directly modulated ROF link for wireless access". In *IEEE Canadian Conference on Electrical and Computer Engineering*, volume 4, pp. 2167–2170, Corfu, Greece, May 2004.

[99] J. E. Mitchell. "Performance of OFDM at 5.8 GHz using radio over fibre link". *Electronics Letters*, vol. 40, no. 21, pp. 1353–1354, Oct. 2004.